SIDEROPHORE-MEDIATED IRON TRANSPORT APPARATUS
IN Paracoccus denitrificans

By

JOHN B. DIONIS

A DISSERTATION PRESENTED TO THE GRADUATE SCHOOL
OF THE UNIVERSITY OF FLORIDA IN
PARTIAL FULFILLMENT OF THE REQUIREMENTS
FOR THE DEGREE OF DOCTOR OF PHILOSOPHY

UNIVERSITY OF FLORIDA

1987

For their continual advice and support, this dissertation is proudly dedicated to my mother and father. Their guidance over the years has proven invaluable in reaching this point in my career.

ACKNOWLEDGMENTS

TABLE OF CONTENTS

iv

Abstract of Dissertation Presented to the Graduate School
of the University of Florida in Partial Fulfillment of the
Requirements for the Degree of Doctor of Philosophy

SIDEROPHORE-MEDIATED IRON TRANSPORT APPARATUS
IN Paracoccus denitrificans

By

JOHN B. DIONIS

August 1987

Chairman: Dr. Raymond J. Bergeron
Major Department: Medicinal Chemistry

The high affinity iron assimilation system in Paracoccus deni-
trificans involving its siderophore parabactin and the cognate membrane
receptor is examined. Parabactin was shown to deliver iron to the
microorganism via an "iron-taxi" mechanism in which the siderophore
iron complex binds to a membrane receptor where the iron is released
and transported into the cell. The deferrated ligand remains extracel-
lular and can be re-utilized in iron transport. The data also indicate
that Paracoccus denitrificans exhibits stereospecificity in its sidero-
phore requirement. The ferric L-parabactin chelate was most effective
in supplying iron to the microorganism. The ferric D-parabactin che-
late was unable to effectively supply iron to the microorganism in
various experimental protocols including growth and transport studies.

The synthesis of parabactin azide, the first catecholamide sider-
ophore photoaffinity label, is described. The photoaffinity label is
shown to have the same biological activity as parabactin in stimulating

v

the growth of Paracoccus denitrificans under low iron conditions. The photoaffinity label was employed in the identification of the siderophore membrane receptor. Additionally, the synthesis of amino parabactin, which is subsequently attached to an activated sepharose resin to produce the first polyamine siderophore affinity column, is described.

The role of isolated Paracoccus denitrificans membrane proteins in siderophore-mediated iron transport is examined. High affinity, stereospecific binding activity for ferric L-parabactin is shown to be associated with the cell membrane and not with the cytoplasmic proteins. An outer membrane preparation from cells grown in low iron medium was found to retain ferric parabactin binding activity following solubilization in a detergent containing buffer. Binding activity was measured by means of a column-centrifugation technique which separated free and receptor bound ferric parabactin. The presence of low-iron inducible high molecular weight proteins as a major component in the solubilized outer membrane preparation containing the highest binding activity indicates that one or more of these proteins is involved in the siderophore-mediated iron uptake system as a receptor for ferric L-parabactin.

Microbial Iron Assimilation

Despite the fact that iron is one of the most abundant metals on earth, nearly all life forms have had to develop sophisticated mechanisms for its access and assimilation. This is due, in part, to the extreme insolubility of ferric ion at physiological pH (K_{sp} of $Fe(OH)_3 = 10^{-38}$ M^{-1})[1] and the tendency of ferric hydroxide to polymerize and precipitate as an oxyhydroxide polymer. It is also evident that the uptake of this metal needs to be regulated at the membrane level as a consequence of the role that iron plays in generating hydroxy free radicals in the presence of hydrogen peroxide.[2]

Iron plays a crucial role in many biological redox systems.[3-5] This is due to the generation of a large redox potential between the interchange of the ferrous and ferric forms, an oxidation state which is very sensitive to both pH and chelation. Iron plays a critical role in the energy requirements of virtually all microorganisms. An excess of the metal causes a fulminant growth of many microorganisms while iron deprivation can substantially slow or even halt growth.[6-8] The respiratory chains of aerobic and facultative anaerobic bacteria have in common the presence of cytochromes and non-heme enzymes, each with a specific requirement for iron.[9] In addition, there are other electron transfer proteins, such as the hydrogenases, iron-sulfur proteins and dehydrogenases which have an absolute requirement for iron. As a

1

means to protect the cell, there are also microbial iron enzymes responsible for the metabolism of hydrogen peroxide and oxygen. These include the catalases, peroxidases, oxygenases as well as certain forms of superoxide dismutase. Other crucial roles which iron plays in bacterial metabolism include the nitrogenase enzyme involved in the fixation of dinitrogen, the aconitase enzyme of the citric-acid cycle and ribonucleotide reductase which is required for DNA synthesis.[9]

The question arises as to why iron was incorporated into so many important enzyme systems in virtually every type of living cell. Iron is the fourth most abundant element on earth, surpassed by only oxygen, silicon and aluminum. It is speculated that iron was firmly established as a bioessential element during the anaerobic phase of life on earth.[10] During this stage of evolution, in which iron was in the readily soluble ferrous form, there would be no need for specific iron-binding compounds. However, when photosynthetic organisms began producing oxygen, the soluble iron was transformed to its insoluble ferric form. This imposed severe restrictions on iron availability and as a result microorganisms developed the means for retrieving iron from insoluble polynuclear complexes and for the delivery of iron to the cell, where it can be processed for use in cellular metabolism. Microorganisms have evolved a group of low molecular weight, virtually ferric ion specific ligands or siderophores to sequester exogenous ferric ion and facilitate the transport of this metal into the cell.[9-12]

In general, siderophores are classed as either hydroxamates,[13] such as desferrioxamine[14] or as catecholamides,[15] as exemplified by enterobactin[16] and the linear catecholamide parabactin[17] (Fig. 1-1). Both desferrioxamine and parabactin form extremely tight complexes
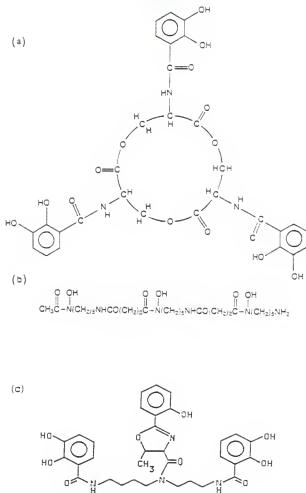
Figure 1-1. Structures of the siderophores. (a) Enterobactin, (b) desferrioxamine and (c) parabactin.

with ferric ion, with formation constants, K_f, of 10^{31} M^{-1} and 10^{48} M^{-1}, respectively.[18,19] Enterobactin, which is a cyclic trimer of 2,3-dihydroxybenzoyl serine, is produced by most enteric species including Escherichia coli and Salmonela typhimurium.[16] The iron (III)-enterobactin formation constant has been calculated to be 10^{52}, making this siderophore the strongest ferric ion chelating agent known.[20] Despite considerable structural variation between the classes of siderophores, a common feature of these ligands is their ability to bind ferric ion in a hexacoordinate, octahedral complex with formation constants in the range of 10^{30}–10^{50} M^{-1}. Moreover, both the hydroxamate and catecholamide siderophores utilize bidentate oxygen containing moieties to form tight complexes with iron (III). The iron (III) being a powerful lewis acid due to its high charge to size ratio forms very stable bonds with the weakly polarizable oxygen atoms.[21]

It is generally found that fungi produce siderophores of the hydroxamate variety, while bacteria frequently produce catecholamide siderophores in addition to hydroxamates. For example certain strains of E. coli produce the catecholamade siderophore enterobactin as well as the hydroxamate siderophore aerobactin.[22] There are also certain siderophores namely mycobactins in which hydroxamate and phenolate ligands are present in the same molecule.[23] The gram-negative soil bacterium Paracoccus denitrificans produces the catecholamide siderophore parabactin. This was the first siderophore isolated which was predicated on a polyamine backbone, in this case spermidine.[24] To each of the triamine nitrogens is affixed a bidentate ligand. The

terminal primary amino groups of the spermidine backbone have 2,3-dihydroxybenzoyl moieties attached while the secondary nitrogen has a 2-(2-hydroxy phenyl)-4-carboxyl-5-methyl-2-oxazoline functionality fixed. The original structure assigned by Tait was inaccurate in that the suggested secondary N-functionality was given as N-(2-hydroxybenzoyl)-L-threonine. It was only later that the functionality was demonstrated to be an oxazoline ring.[25] The soil bacterium _Agrobacterium tumefaciens_[26] produces the catecholamide siderophore, agrobactin (Fig. 1-2). This ligand is nearly identical to parabactin but it contains an additional hydroxyl on the central aromatic ring. Another hexacoordinate polyamine catecholamide siderophore has been isolated from the cultures of _Vibrio cholerae_.[27] This ligand, known as vibriobactin (Fig. 1-2), is predicated on the less frequently found symmetrical norspermidine backbone and has in common with the previous two siderophores a phenyl oxazoline ring system in which the oxazoline nitrogen is utilized in iron chelation. It should be noted that the synthesis of the above mentioned polyamine catecholamide siderophores has been accomplished in our laboratories.[28-30]

Another interesting feature of the hydroxamate and catecholamide ligands is that the siderophore iron complex can exist in two different optical configurations arising from chelation of the metal in either a left-handed Λ, or right-handed Δ, "coordination propeller" (Figs. 1-3 and 1-4).[9] This can be visualized as one bidentate ligand being set in a potentially preferred spatial orientation. The remaining two bidentate ligands could then cluster around the iron in either the Λ or Δ-coordination.

(a)
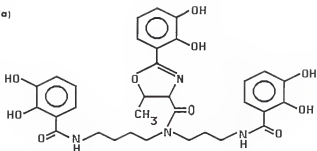
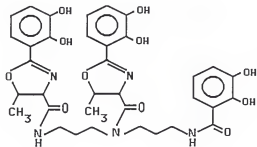(b)

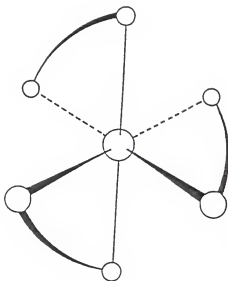Figure 1-2. Structures of the siderophores. (a) Agrobactin and (b) vibriobactin.

Λ

Figure 1-3. Representation of the Λ coordination isomer.

Δ
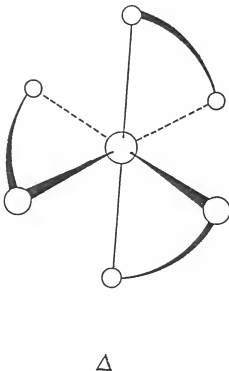
Figure 1-4. Representation of the Δ coordination isomer.

It is very interesting that the specific iron-siderophore transport systems present in microbial species recognize only the siderophore with the appropriate chirality about the iron center. The implications are that by producing siderophores from optically active components, microorganisms have found a way to monopolize iron in a competing environment. In other words, they can excrete siderophores which are only recognizable to their own transport systems. The major criteria for survival in this competing environment would then be the ability to synthesize a chelator with a higher affinity for iron. It would also be expected that those species which have evolved more than one mechanism of iron-transport would be better suited for survival. It should be pointed out that certain bacteria have evolved specific transport systems for siderophores produced by other microorganisms. For example, the enteric bacteria $\underline{E.\ coli}$ possesses a transport apparatus for the siderophore ferrichrome.[31] This hydroxamate siderophore, which $\underline{E.\ coli}$ does not synthesize, is produced by many species of fungi and was first isolated by Neilands from the mycelium of the smut fungus $\underline{Ustilago\ sphaerogena}$.[32]

The concentration of iron required for maximal growth of most gram-negative bacteria in culture ranges from 0.02 to 0.1 µg/mL.[33] These iron requirements are influenced by a number of different factors. Strongly aerobic organisms such as Pseudomonas, Azotobacter and Mycobacterium have much higher iron requirements, approaching 5 µg/mL.[33] A species of blue green algae, $\underline{Nostoc\ muscorum}$, required 10 µg Fe/mL for maximal fixation of dinitrogen.[34] It has been shown that higher iron concentrations are required by microorganisms growing in an environment containing metals such as Al^{3+}, Cr^{3+} or Cu^{2+}.[35,36]

These metal ions can directly interfere with bacterial assimilation of iron as they bind effectively to siderophores. The bacterial requirement for iron is also very sensitive to temperature. Studies indicate that with increasing temperature there is a drastic reduction in siderophore biosynthesis.[37,38] This results in an increased iron requirement, as the microorganism can no longer transport this vital metal using its high affinity system. In *Salmonella typhimurium*, a pathogenic bacterium which also produces the catecholamide siderophore enterobactin, the concentration of iron required for maximal growth was determined to be 0.1 µg/mL at various temperatures, ranging from 31° to 36.9°C.[37] However, when the incubation temperature was raised to 40.3°C there occurred a concomitant loss of enterobactin synthesis and an increase in the iron requirement for maximal growth by nearly 30 fold. As this critical temperature is within the range of most physiological systems, it has been speculated that fever may play an important role in the control of pathogenic microorganisms. By raising the temperature to the critical point, the biosynthesis of iron transport compounds could be turned off, resulting in the loss of the microorganisms' ability to compete for iron present in the host.

The virulence of many pathogens is dependent upon interactions between host and pathogen. Indeed it is becoming more and more evident that the virulence of many bacteria can be directly associated with the production of siderophores thus implicating iron assimilation as a critical component in the host-pathogen interchange.[39,40] The availability of iron in the tissues of the mammalian host is severely restricted.[41] The majority of the total body iron is found intracellularly as ferritin, hemosiderin and hemoglobin. The small quantity

which is extracellular and potentially available to invading pathogens is tightly bound by high affinity iron-binding glycoproteins. Transferrin, the iron binding protein of serum, and lactoferrin, a similar protein found in secretions, are normally unsaturated and limit the availability of iron necessary for microbial growth to 10^{-12} M or less.[42] The ability of microbial pathogens to aquire iron in a host is one factor determining the virulence of a microorganism and is considered a prerequisite to infection.

In many cases the more virulent strains in a given species are those which contain multiple pathways for the assimilation of iron. The virulence factor in invasive strains of E. coli is not the expected catecholamide siderophore enterobactin but the hydroxamate siderophore aerobactin.[43] At first glance this appears to be a contradiction as the metal binding affinity of aerobactin is far inferior to enterobactin at physiological pH. An explanation implicating the role of serum albumin on siderophore-mediated utilization of transferrin iron has been advanced by Konopka and Neilands.[44] Their initial results demonstrated that the abilities of the siderophores enterobactin and aerobactin to remove iron from transferrin in vitro were very dependent on the composition of the medium. While the ability for enterobactin to remove transferrin iron was greater in buffer solutions, the transfer rate in serum was far superior for aerobactin.[45] Further studies demonstrated the effects of serum proteins on siderophore mediated utilization of transferrin iron. Serum albumin, the most abundant protein in human plasma accounting for 60% of the total, is known to bind to many hydrophobic ligands.[46] Serum albumin and human serum were shown to be comparable in their selective ability to interfere with

the transfer of iron from ferric enterobactin to E. coli. Furthermore, serum albumin was shown to bind enterobactin in a 1:1 stoichiometry with a binding constant greater than 10^4 M^{-1}.[45] In contrast, aerobactin had no detectable affinity for serum albumin and was able to transfer iron to the cells in the presence of serum albumin. The explanation for this behavior is probably best attributed to the different chemical structures of the two siderophores. The catecholamide siderophore enterobactin is a lipophilic molecule possessing 2,3-dihydroxybenzoic acid moieties. This aromatic character results in a susceptibility of the siderophore to bind to serum proteins. This tendency could also result in the formation of antibodies to the siderophore. Evidence for the presence of enterobactin specific antibodies has been reported.[47] An immunoglobulin A antibody isolated from human serum was shown to inhibit uptake of iron from enterobactin but not from ferrichrome or citrate.[48] These results suggest that the synthesis of aerobactin is an important factor in the virulence of invasive strains of E. coli. Aerobactin has the ability to remove transferrin bound iron in the presence of serum proteins and to deliver the metal to the invading pathogen.

Structural Organization of the Bacterial Cell Envelope

An examination of bacterial iron transport cannot be complete without a general background into the structural organization of the gram-negative bacterial cell envelope. This complex envelope consists of various layers with distinct chemical compositions which impart markedly different physical characteristics to each.[49] These layers are associated with one another through various points of attachment and hence the function of each layer is modified by other cell wall

components. An interesting feature of the cell envelope is its contin-
ual synthesis in response to cell growth. In fact, the outer membrane
is a classic example of membrane biogenesis in which all major constit-
uents are synthesized elsewhere in the cell.[50] Assembly of the
membrane requires translocation and insertion of each component into
the final membrane structure.

It is at the inner or cytoplasmic membrane that the structural
components of the cell wall are synthesized.[51] These various com-
ponents include the basic chemical units of peptidoglycan, lipopolysac-
charide and phospholipid. The cytoplasmic membrane is a phospholipid
bilayer containing a large number of peripheral and integral pro-
teins.[52] The cytoplasmic membrane also functions in the active
transport of substrates, including iron. Inner membrane vesicles from
cells of E. coli have been shown to transport $[^3H]$-ferrichrome with a
K_m of 0.2 μM.[53] The transport mechanism indicated an energy dependence
as detected through the use of metabolic inhibitors as well as a need
for divalent cations.[54]

The peptidoglycan is an essential feature in all bacteria albeit
in highly variable amounts. This structure surrounds the bacterial
cytoplasmic membrane and prevents cell lysis in hypotonic environments
as well as contributes to cellular form and rigidity.[55] It has also
been shown that the peptidoglycan is closely associated with the outer
membrane. A specific lipoprotein, covalently linked to the peptidogly-
can, extends outward towards the outer membrane and serves to anchor
the membrane by hydrophobic interactions with the phospholipids present
in the outer membrane.[56] Due to a lack of extensive cross-linking,

the peptidoglycan of gram-negative bacteria does not constitute an effective barrier to the passage of small molecules.

The area between the cytoplasmic membrane and the outer membrane of gram-negative bacteria is known as the periplasmic space. This area serves a similar function as the eukaryotic lysosome, which houses the hydrolytic enzymes such as the proteases, lipases, phosphatases and nucleases.[57] Bacteria, however, do not contain lysosomes and in order to prevent self-degradation have maintained these enzymes separate from other cell components in the periplasmic space. This space, which can comprise nearly 30% of the total cell mass, is also involved in transport. Specific binding proteins associated with the outside of the cytoplasmic membrane, transport amino acids and sugars through the cytoplasmic membrane into the cell. Thus, periplasmic enzymes can act on a wide variety of substrates which diffuse into this zone and convert them to molecules which are transportable into the cell utilizing the specific binding proteins and permeases.[49] While there is no direct evidence implicating periplasmic binding proteins in siderophore mediated iron transport, their existence cannot be ruled out.

The layer which controls the passage of molecules into and out of the periplasmic space is the "molecular sieve" layer better known as the outer membrane. This layer, which is an asymmetric bilayer, is composed mainly of lipopolysaccharide, phospholipid and protein.[58] The lipopolysaccharide, comprising as much as 45% of the outer membrane, is responsible for antigenicity, binding of specific enzymes and contributes to the hydrophobicity of the outer membrane.[59] It is the lipopolysaccharide which to a major extent protects enteric bacteria

from lysis due to exposure to bile salts in the intestinal flora of animals.

The outer membrane is made up of several major and minor proteins. However, a minor protein can, under certain growth conditions, be made in quantities as great as that of major proteins. Another interesting property of the outer membrane is the nonspecific permeability toward small, hydrophilic substances. The outer membrane can thus provide specific and nonspecific channels for nutrients and ions required for growth. Matrix proteins known as "porin" function to form such passive diffusion pores throughout the outer membrane.[60] The porins render the outer membrane freely permeable towards hydrophilic molecules (<650 Mw) such as sugars, amino acids and peptides.[21] These major proteins are characterized by a tight, noncovalent association with the peptidoglycan, presumably through electrostatic forces. They are also unique in containing a high content of β-structure in contrast to other intrinsic proteins. It is of interest that these essential proteins located on the cell surface have become the target for various phages.

It has been shown that in many bacterial species there are outer membrane proteins which function as receptors in the uptake of ferric ion siderophore complexes.[52] These receptor proteins are produced concomitantly with iron deprivation and bacterial siderophore production. Characterization of these proteins by sodium dodecyl sulfate polyacrylamide gel electrophoresis (SDS-PAGE) indicates a molecular weight in the range of ca. 80,000 daltons for the ferrichrome and enterobactin receptor proteins of E. coli.[52] It is postulated that

these proteins may contact the cytoplasmic membrane at various adhesion zones. Indeed, the ferrichrome receptor has been shown to be located at such an area.[52] The primary function of these receptor proteins is the initial binding of the siderophore-metal complex. After this step, there are a number of different scenarios which one could envision. One such scenario would have the ferric siderophore complex translocated into the cell, perhaps to the site of the cytoplasmic membrane, facilitated via an adhesion zone. At this point, a specific binding protein would transport the siderophore-chelate into the cytoplasm where the metal ion would undergo a reductive separation from the ligand. Obviously, there can be a number of variations to this scenario. The most striking being that release of iron from the siderophore occurs at the membrane level. In this way, siderophore uptake is not required for transport of the metal.

From the aforementioned discussion it is clear that iron acquisition plays a critical role in the survival of microbial species. The mechanism by which microorganisms compete for this vital metal has been the subject of intensive research. It is hoped that the research presented herein will contribute to the better understanding of microbial iron transport.

CHAPTER II
Paracoccus denitrificans IRON TRANSPORT APPARATUS

Introduction

Due to the physiological importance of iron coupled to its
extreme insolubility at physiological pH, living organisms have evolved
diverse pathways for iron assimilation. When confronted by iron-
deficient conditions, microorganisms synthesize low molecular weight
ferric ion chelating agents called siderophores. The siderophore and
the matching membrane-associated receptor which recognizes the ferric
chelate comprise the "high affinity" iron transport system in micro-
organisms.[9] It is this high affinity iron transport pathway which has
received considerable attention. Less is known concerning the rela-
tively inefficient "low affinity" transport system of microbial iron
uptake. In this process it is believed that microorganisms have the
ability to utilize ferric ion without the necessity for synthesizing
specific siderophores and their corresponding membrane receptors for
the solubilization and transport of this metal. The concentration of
utilizable iron in the cell environment must be relatively high on the
order of 10 μM for maximal growth.[9]

In the present study we examine the high affinity system by
which Paracoccus denitrificans utilizes its siderophore parabactin in
its iron-transport apparatus. The effects of D-parabactin, L-para-
bactin, and citrate on the growth of Paracoccus denitrificans in iron
deficient media were determined. The results demonstrate the presence
of a stereospecific iron transport apparatus inducible by a low

17

concentration of utilizable ferric ion in the cell medium. Additionally, the mechanism by which <u>Paracoccus denitrificans</u> utilizes its siderophore to supply iron to the cell is examined.

Materials and Methods

Culture Media and Glassware

Water was purified by distillation in a Mega-pure still (Corning) and passed through a deionizing filter (Sybron-Barnstead) prior to use. All glassware was soaked in 3N hydrochloric acid for at least 1 h and rinsed well with purified water.

Liquid culture medium contained per liter of water the following: 13.5 g of sodium succinate, 4.0 g of KH_2PO_4; 4.9 g of Na_2HPO_4; 1.6 g of NH_4Cl; 0.4 g of $MgSO_4/7H_2O$; 1% v/v Tween 80 and 4.5 µmol $MnSO_4$. The pH was adjusted to 7.0 with 5 M NaOH and filter sterilized through a 0.22 µ filter (Milipore). Atomic adsorption analysis indicated 2.0 µM iron present in this culture medium.

Growth Studies

Iron-free ligands were added in methanol to empty, sterile Klett flasks, evaporated to dryness under nitrogen passed through a 0.22 µ Millipore filter and redissolved in the sterile growth medium. In addition ethylenediamine-di(O-hydroxyphenylacetic acid) (EDDA) and Fe $(NO_3)_3$ were added to the liquid culture medium in each experiment as required to maximize differential growth response to the various ligands. Inoculations from a 24 h trypticase soy broth culture were made into the liquid culture medium at 40 µL of broth per 10 mL of culture medium and incubated with shaking at 30°C. Growth rates were determined by monitoring Klett readings vs. time. Standard curves were generated correlating Klett units with colony forming units using serial plating techniques. Growth studies were reported as CFU's vs. time.

Transport Assays

Individual colonies of Paracoccus denitrificans were inoculated into 20 mL of trypticase soy broth and incubated for 24 h at 30°C with rotary shaking. Inoculations were then made into liquid culture medium at 20 µL of broth per 10 mL of culture media and incubated with rotary shaking at 30°C. Cells were harvested after 48 to 72 h by centrifugation at 5000 g for 20 minutes at 4°C, washed twice with cold culture medium and resuspended in fresh culture medium to a Klett reading of 150. Stock solutions of [^{55}Fe] and [^{3}H] labeled chelates in Tris HCl buffer pH 7.5 were added to the cell suspensions and incubated with rotary shaking at 30°C. At various time points, aliquots were removed (200 µL) and immediately diluted with cold culture medium (5 mL). This mixture was then rapidly filtered through a Gelman GA-6 membrane filter. The filters had been presoaked for 24 h in a 1 mM unlabeled chelate solution to decrease adsorption of the radiolabeled chelate to the filters and were rinsed once with culture medium (5 mL) before filtering the cell suspensions. After the cells had been collected, the filters were rinsed with cold culture medium (5 mL). Liquid scintillation counting of the air-dried filters was then performed in 10 mL of Biofluor cocktail. Control values of labeled chelates adsorbed to the filters in the absence of cells were determined, then subtracted from the values obtained with cells present. Uptake of labeled chelates by cell suspensions of Paracoccus denitrificans is presented as "percent uptake," which indicates the percentage of the total amount of added label that has been taken up by the cells.

Results

Various organic acids such as citric, succinic and malic, have been suggested to play a role in iron metabolism. When the tricarboxylate citrate was used in relatively high concentrations it can furnish _E. coli_ with iron in an apparent high affinity system.[61] An 80,500 molecular weight outer membrane protein is expressed which has been shown to be a specific ferric citrate receptor.[61] It appears that citrate may also act as a low affinity transport system in other microorganisms as seen in the mycobacteria. While it was shown that ferric citrate could promote the growth of the microorganism, there was no evidence for the induction of specific membrane proteins.[62]

An experiment was performed to determine whether citrate was capable of supplying iron to _Paracoccus denitrificans_. We compared the effects of citrate and L-parabactin on the growth stimulation of _Paracoccus denitrificans_ in liquid culture media containing the synthetic iron chelator EDDA. This chelator forms an iron complex which the microorganism cannot utilize and hence results in a medium which is severely lacking in any utilizable free iron. Figure 2-1 compares the ability of citrate and L-parabactin, present at 0.8 μM, in promoting the growth of the microorganism. It can be seen that the addition of L-parabactin produced a significant enhancement in growth rate when compared to citrate or controls throughout the experimental period. Citrate was incapable of facilitating stimulation of microbial growth under these experimental conditions. The growth stimulation from L-parabactin was expected, since this is the siderophore which
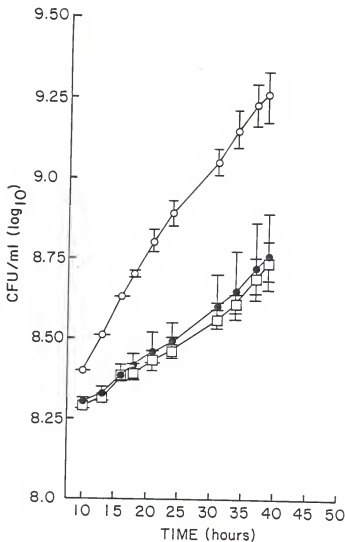
Figure 2-1. Growth rate of _Paracoccus denitrificans_ in the presence of L-parabactin (O) (0.8 μM), citrate (●) (0.8 μM), or controls (□).

Paracoccus dinitrificans produces under low iron conditions. To deter-
mine whether Paracoccus denitrificans displays any stereospecificity in
its ferric parabactin-mediated iron-transport system, L-parabactin and
its enantiomer D-parabactin were compared for their ability to stimu-
late microbial growth. Both ligands would be expected to compete very
effectively for iron chelated to EDDA. In addition the iron (III) for-
mation constant for L-parabactin would be identical with that of the
enantiomeric form of parabactin. In this way any differences in growth
stimulation could be directly attributed to cell recognition of the
isomer with a preferred coordination about the metal center. High
field ^{1}H NMR studies of the gallium (III) complex of L-parabactin and
the circular dichroism spectrum of the ferric siderophore indicate that
ferric L-parabactin exists in solution as the Λ-coordination isomer to
the exclusion of the Δ isomer.[63,64] In contrast, by substituting
D-threonine into the synthetic scheme one produces the enantiomeric
form of parabactin which will chelate ferric ion to form the Δ coordin-
ation isomer to the exclusion of the Λ isomer.

Figure 2-2 demonstrates the effects of 20 µM L-parabactin and
D-parabactin on the growth of liquid cultures of Paracoccus denitrifi-
cans. Again, the addition of L-parabactin at the time of inoculation
resulted in a stimulation of growth throughout the experimental period.
In contrast, D-parabactin was much less efficient in stimulating the
growth of the microorganism compared to L-parabactin. However, there
was a slight growth stimulation in the presence of D-parabactin when
compared to controls. In this experiment the concentration of EDDA
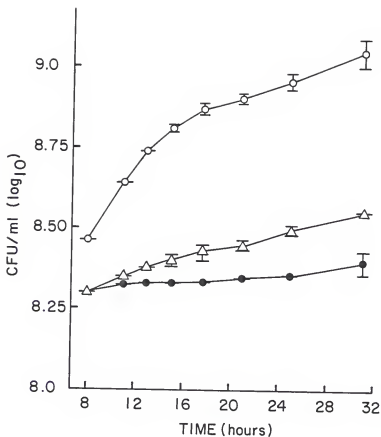
Figure 2-2. Growth rate of _Paracoccus denitrificans_ in culture media containing ferric nitrate (0.05 μM) with L-parabactin (O) (2.0 μM), D-parabactin (Δ) (2.0 μM), or no carrier (●).

in the liquid culture medium was 0.55 mM while the concentration of
ferric nitrate was 0.05 µM. It appears likely that under these condi-
tions D-parabactin is operating via a mechanism other than the high
affinity iron uptake system. A possible explanation is that a slow
diffusion process is occurring whereby the hydrophilic D-parabactin
ferric chelate passes across the outer membrane of the microorganism
into the cell. This would not be expected to occur to any substantial
degree as the molecular weight of the ferric complex is very near the
exclusion limit of porin structures present in the outer membrane of
gram-negative bacteria.[65] However, over the time course of the
experiment (ca. 32 h), small amounts amounts could conceivably pass
through the outer membrane and provide iron to the cell.

In a similar experiment, we compared the ability of L-parabactin
and D-parabactin to stimulate the growth of Paracoccus denitrificans
under severe iron deprivation conditions (Fig. 2-3). In this experi-
ment the concentration of EDDA present in the media was doubled and
ferric nitrate was omitted. The results from this experiment indicate
quite conclusively that Paracoccus denitrificans displays stereospec-
ificity in its siderophore-mediated iron transport apparatus. Only
L-parabactin was able to effectively stimulate growth throughout the
experimental period. Under these experimental conditions D-parabactin
was ineffective in facilitating growth stimulation as compared to con-
trols. This enantiomeric form of parabactin may be able to function
only as a low affinity iron transport system, and therefore be incap-
able of producing growth stimulation at the extremely low available
iron concentration present in this experiment. Only when there is
increased iron availability does one observe a growth stimulation
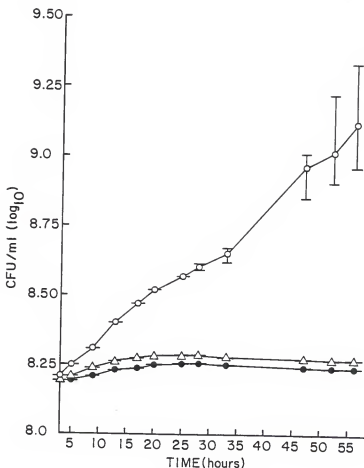effect from D-parabactin.

Figure 2-3. Growth rate of Paracoccus denitrificans in the presence of L-parabactin (○) (2.0 μM), D-parabactin (△) (2.0 μM), or controls (●) without added ferric nitrate.

We have recently examined the mechanism by which *Paracoccus denitrificans* utilizes its siderophore L-parabactin in its iron transport apparatus.[19,66] Siderophore-mediated iron transport was investigated by incubating cell suspensions with the ferric complex of L-parabactin in which radiolabel was present either on the ligand or on the metal. In this way it would be possible to differentiate between the uptake of intact siderophore-metal complex "versus" uptake of iron without corresponding accumulation of ligand. To monitor the fate of radiolabeled metal, cell suspensions of *Paracoccus denitrificans*, grown under iron deficient conditions, were presented with [^{55}Fe]-ferric L-parabactin at 1.0 μM and incubated with rotary shaking at 30°C. Aliquots were removed at various time points, then filtered through a 0.45 μ filter which was housed in a vacuum manifold system. After rinsing, the filters were dried and the retained Fe was determined by scintillation counting. The incorporation of radiolabeled metal continued throughout linearly for 1 h and then leveled off at approximately 50% of the total amount of radiolabel (Fig. 2-4). To determine whether uptake of siderophore was occurring with uptake of iron, cells were presented with the iron complex of the radiolabeled ligand [^{3}H] L-parabactin. In contrast to the rapid incorporation of radiolabeled metal from [^{55}Fe] ferric L-parabactin, there was no appreciable uptake of labeled siderophore in cells incubated with [^{3}H] ferric L-parabactin (Fig. 2-4). In both instances a small percentage of radiolabel (10%) was associated with the cells at the earliest time points. However, only in the case where cells had been incubated with
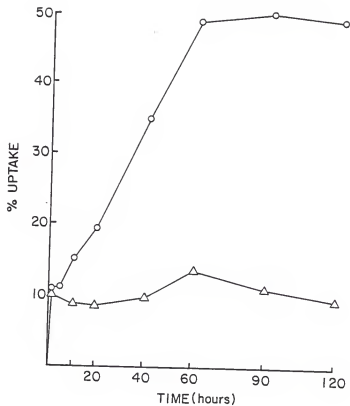
Figure 2-4. Uptake of [^{55}Fe] ferric parabactin (O), and [^{3}H] ferric parabactin (Δ) by <u>Paracoccus denitrificans</u>.

the [^{55}Fe]-labeled siderophore was additional uptake of radiolabel
observed.

The previous data showed that Paracoccus denitrificans exhibits
stereospecificity in its siderophore requirement under low iron condi-
tions. To further demonstrate stereospecificity in its iron transport
apparatus [^{55}Fe] ferric L-parabactin and its enantiomer [^{55}Fe] ferric
D-parabactin were compared for their ability to donate iron to the
microorganism (Fig. 2-5). When cells were presented with [^{55}Fe] ferric
L-parabactin there was, as expected, a rapid incorporation of radio-
labeled metal which had maximized after 60 min into the experiment. In
contrast, when cells were presented with [^{55}Fe] ferric D-parabactin
there was no appreciable uptake of radiolabel in comparison to that
which was already cell-associated within the first minute of the assay.
It is thus apparent that enantioparabactin is incapable of supplying
iron to Paracoccus denitrificans in a high affinity transport system.

Discussion

Considering the number and diversity of the iron specific sidero-
phores, it is not surprising that there are indeed a variety of mechan-
isms of microbial iron transport. Four such mechanisms have been elu-
cidated by which siderophores facilitate microbial iron assimilation.

In the "iron-taxi" delivery system[67-69] the siderophore iron com-
plex binds to a specific membrane receptor protein in a temperature
independent step. The metal is then released from the ferric-sidero-
phore receptor complex to a presumed iron binding acceptor protein
which facilitates the transfer of iron into the cell. The deferrated
ligand, no longer having a high affinity for the specific binding pro-
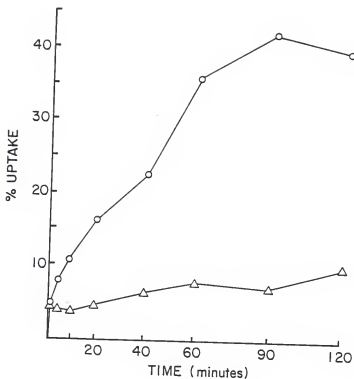tein, would then be displaced by another ferric siderophore molecule.

Figure 2-5. Uptake of [^{55}Fe] ferric parabactin (O), and [^{55}Fe] ferric enantioparabactin (△) by <u>Paracoccus denitrificans</u>.

The striking feature of the "iron-taxi" mechanism is that incorporation of iron into the cell does not occur concomitant with siderophore transport. In this way the siderophore remains extracellular at all times allowing the siderophore to be reutilized in iron transport.

The more common mechanism of bacterial and fungal iron assimilation is known as the "iron shuttle" delivery system.[70,71] The noteworthy feature of this scheme is the transport of the intact siderophore-iron complex, followed by intracellular dissociation of the metal-ligand complex. The initial step in the "iron shuttle" mechanism, not unlike the "iron-taxi," involves the temperature-independent binding of the siderophore metal complex to a specific membrane receptor protein. The next step, in contrast to the "iron-taxi," involves the translocation of the intact siderophore metal complex into the cell, presumably to the site of the cytoplasmic membrane. Specific binding proteins, located at the surface of the cytoplasmic membrane, then transport the siderophore metal complex into the cytoplasm where the metal ligand complex is dissociated. There have been two mechanisms advanced describing the fate of the intracellularly released ligand. In the "European mechanism," the subsequent step involves a translocation of deferrated ligand from the cytoplasm to the extracellular environment.[67] In this way the ligand can be reused to supply iron to the cell. In the "American mechanism," after intracellular release of siderophore bound iron, the ligand is degraded intracellularly.[72] The ligand degradation products are then released into the extracellular medium.

A very pertinent example of iron transport mechanisms occurs in the fungus Ustilago sphaerogena. This organism has evolved the means for incorporation of iron by utilizing the hydroxamate siderophores ferrichrome and ferrichrome A which it biosynthesizes. The trihydroxamate siderophore ferrichrome donates iron to the cells in an apparent "iron-shuttle" delivery system while the siderophore ferrichrome A operates by the "iron-taxi" mechanism.[70,73] Before embarking on the specifics of iron-transport in this system, it should be pointed out that fungi are eukaryotic organisms and as such do not contain an outer-membrane as found in the prokaryotic bacteria. Instead, they possess a single cytoplasmic membrane which is surrounded by a hyphal wall. In fungi, the receptors and iron-transport system are located at the cytoplasmic membrane.[74]

In a double label experiment, Emery demonstrated that in the case of ferrichrome, both ligand and metal were initially accumulated at the same rate into the cell.[69] When presented with $[^{14}C]$ and $[^{59}Fe]$-labeled ferrichrome, cell suspensions of Ustilago sphaerogena rapidly incorporated label over the first 60 min of the experiment. At this point in the experiment, the cells had taken up nearly 70% of the total amount of ^{55}Fe and ^{14}C radiolabel present in the culture medium. Interestingly, as the experiment progressed, there occurred a slow-release of $[^{14}C]$-labeled deferri-ferrichrome back into the culture medium. This expulsion of deferrated ligand occurred until the percent uptake had leveled off at approximately 40% of the total amount of radiolabel present. In contrast, there was a continued uptake of metal from $[^{59}Fe]$-labeled ferrichrome which maximized near 100% uptake after 2 h.

To further investigate the mechanism of ferrichrome-mediated iron-transport, the effects on cells incubated with the aluminum chelate of [^{14}C]-labeled deferri-ferrichrome were examined.[69] Aluminum forms a trivalent cation with a similar size radius as compared to that for iron (III). As one might expect aluminum possesses a high affinity for siderophores. Emery demonstrated that cell suspensions of Ustilago sphaerogena rapidly incorporated the intact [^{14}C]-ferrichrome Al (III) chelate. Additionally, there was a marked absence of the release of [^{14}C]-ferrichrome back into the culture medium as was shown to occur when the [^{14}C]-ferrichrome iron complex was presented to the cells. These results are in keeping with the proposed "iron-shuttle" mechanism in which the metal and siderophore are taken up at identical rates. After iron removal presumably by a reduction step, the free ligand is expelled and reappears in the extracellular environment. In the case of ferrichrome, the siderophore is released back into the culture medium in unaltered form so that it may be reutilized in iron transport, as in the "European mechanism." In the case of the aluminum chelate of ferrichrome, the organism lacks a mechanism to remove the metal from the stable aluminum complex so that release of free ligand back into the culture medium does not occur.

Ecker and Emery have also investigated the ferrichrome A mediated iron transport system in Ustilago sphaerogena.[70] By utilizing double label transport assays with iron and gallium siderophore complexes, it was determined that ferrichrome A was operating via an "iron-taxi" mechanism. Whereas the [^{14}C]-labeled ferrichrome iron-complex was rapidly incorporated into the cells, there was no appreciable uptake (<5%) of the [^{14}C]-labeled ferrichrome A iron-complex. In contrast,

when [^{59}Fe]-labeled ferrichrome A was presented to the cells there was observed a near quantitative uptake of the metal after 30 min. These results are in keeping with the proposed "iron-taxi" transport mechanism in which only the metal is incorporated by the cells. In this process the siderophore iron complex binds to a membrane receptor where an enzymatic release of iron occurs. The deferrated ligand remains extracellular and can be used again for iron transport.

In their continuing studies, Ecker and Emery witnessed an interesting phenomena when the gallium complex of ferrichrome A was incubated with cells.[70] While gallium (III) is very similar to iron (III) in its coordination chemistry, it does not exist in a stable $^{+2}$ oxidation state.[75] Substitution of iron by gallium would be expected to result in a loss of metal incorporation if the siderophore were operating by an iron-taxi mechanism as enzymatic release of metal will not occur. To the contrary, Emery observed a rapid and quantitative uptake of metal when the [^{67}Ga]-complex of ferrichrome A was presented to the cells. When the [^{14}C]-labeled ferrichrome gallium (III) complex was incubated with the cells, there was also an incorporation of ligand into the cells at a rate identical to the rate of metal uptake. An explanation for these apparent contradictions in the iron-uptake mechanism mediated by ferrichrome A has been advanced. It would appear that the mechanism of iron uptake from ferrichrome A depends upon the ability of the cell to reduce the metal. Under iron-deficient or low aeration conditions ferrichrome A operates by the iron-taxi mechanism. However, if the cell cannot reduce the metal, as is observed under vigorous aeration, the substitution of iron by gallium or under iron-replete conditions, the ligand is accumulated with the metal as an intact complex.

The synthesis of ferrichrome in addition to ferrichrome A affords a strong competitive advantage to Ustilago sphaerogena over other competing organisms under conditions of iron deprivation. The finding that only ferrichrome is synthesized under relatively high iron concentrations (50 µM) suggests a possible role in intracellular iron storage or transport. Interestingly, at concentrations much higher than 10 µM biosynthesis of ferrichrome A is completely shut down. Only under more severe iron deficient conditions is the biosynthesis of this siderophore up-regulated. It is not surprising that ferrichrome A possesses a higher affinity for iron than ferrichrome. This is due to the conjugated nature of its hydroxamate functionalities in addition to the tricarboxylic acid group which aids in lowering extracellular pH.[70] Ferrichrome has been shown to be a potent growth factor in several fungi and bacterial species.[9] Indeed, E. coli produces a specific receptor for ferrichrome. Ferrichrome A, however, does not appear to supply iron to other microorganisms and thus provides another means by which Ustilago sphaerogena can monopolyze iron in a competing environment.

The high affinity iron transport system in Paracoccus denitrificans mediated by the siderophore parabactin appears to operate by the "iron-taxi" mechanism. Cell suspensions grown under iron deficient conditions rapidly incorporate iron when presented with [^{55}Fe]-labeled ferric L-parabactin at 30°C. When cells were incubated with [^{3}H]-ferric L-parabactin there was no appreciable uptake of label at 30°C. In experiments performed at 0°C it was shown that uptake of labeled metal had decreased dramatically, to a value nearly identical

to the [3H]-labeled ligand (Fig. 2-6). The first stage in the iron-taxi mechanism involves binding of the siderophore iron complex to a membrane receptor in a temperature independent step. It would appear that the succeeding step involving iron release from the siderophore-iron complex is impeded at 0°C so that iron transport into the cell does not occur. The possibility still existed that parabactin was operating by a mechanism other than the iron-taxi in delivering iron to the cells. For instance, the parabactin iron complex could be entering the cell intact followed by a rapid expulsion of deferrated ligand. In this manner, the observable uptake of labeled ligand at any specific time point would be negligible. To investigate such a possibility, it was necessary to monitor the fate of the [3H]-labeled L-parabactin gallium (III) chelate. As mentioned previously, gallium does not exist in a stable $^{+2}$ oxidation state. It has been shown that *Paracoccus denitrificans* possesses a reductase capable of removing iron from parabactin. Thus, if parabactin were operating via an iron shuttle mechanism one would expect to see transport of the intact parabactin gallium complex inside the cell. Without a release mechanism for the metal there would be an accumulation of radiolabeled ligand in the cell. Contrary, when cells were incubated with the [3H]-labeled L-parabactin gallium (III) complex, there was observed no appreciable uptake of labeled ligand (Fig. 2-7). The small amount incorporated was identical to that which was cell associated at the earliest time points. Thus it appears very likely that parabactin is operating by an iron-taxi mechanism.

Additionally, the results indicate that the initial step in the binding of the siderophore-iron complex to the cell membrane is a

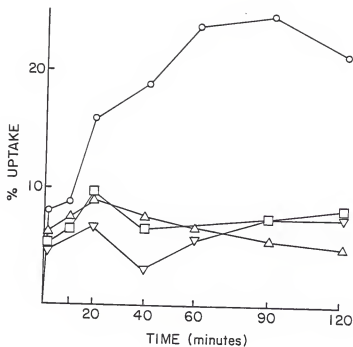Figure 2-6. Uptake of [^{55}Fe] ferric parabactin at 30°C (O) and 4°C (□); [^{3}H] ferric parabactin at 30°C (Δ) and 4°C (▽) by <u>Paracoccus denitrificans</u>.
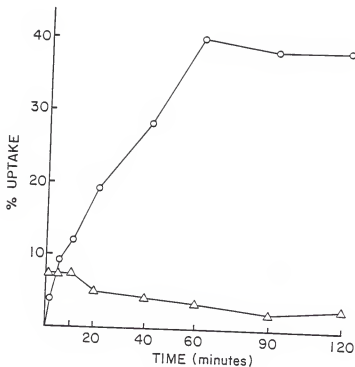
Figure 2-7. Uptake of [^{55}Fe] ferric parabactin (O), and the gallium (III) chelate of [^{3}H] parabactin (△) by _Paracoccus denitrificans_.

specific process. Transport of radiolabeled iron was demonstrated only for cells presented with [^{55}Fe]-L-parabactin. Labeled iron presented in the form of the D-parabactin complex was not transported into the cells. Similar results were obtained when measuring the ability of L- or D-parabactin to stimulate the growth of liquid cultures of Paracoccus denitrificans. Only in the presence of L-parabactin was there considerable growth stimulation from the time of inoculation. Stimulation from D-parabactin was observed only under less severe iron deprivation conditions in an apparent low-affinity transport system. These results suggest that Paracoccus denitrificans recognizes a specific coordination isomer in which the chelating groups are in a left-handed or Λ-coordination propeller about the metal, as in the case of the ferric L-parabactin chelate and is able to discriminate between the mirror image.

The stereospecific uptake of siderophore-iron complexes has also been demonstrated in other microorganisms. There is now substantial evidence that the chirality around the siderophore iron chelate is a major factor that determines recognition of the complex by a specific membrane receptor. Both Neurospora crassa and E. coli have receptor systems which recognize the siderophore ferrichrome.[76,77] This ligand exists in the preferred Λ-coordination isomer. The synthetic enantiomer of ferrichrome which exists in the Δ-coordination isomer was ineffective in supplying iron to the microorganisms. It has also been demonstrated that enantio-enterobactin was ineffective in donating iron to E. coli as compared to the natural siderophore, enterobactin.[76] Various synthetic derivatives of enterobactin, including carbocyclic and

aromatic analogues, were tested to determine the structural boundary conditions which the microorganism sets when utilizing the iron chelate.[78] Changes in the cyclized serine backbone of enterobactin resulted in, surprisingly, only a slight decrease in its ability to donate iron indicating that the chirality about the metal center is the most important factor determining recognition by the bacteria.

Experiments with several parabactin analogues reveal that in Paracoccus denitrificans factors in addition to the chirality about the metal center play a major role in iron transport and recognition.[19] In fact relatively slight changes in the structure of the siderophore were shown to drastically alter the iron-uptake characteristics. For example, homoparabactin which contains a symmetrical 4,4 triamine backbone was investigated for its ability to stimulate growth of the microorganism in liquid culture medium. The results indicated that homoparabactin was far less efficient in promoting growth stimulation under iron deprivation conditions as compared to parabactin. There was, however, an increase in growth as compared to controls in the presence of homoparabactin. This sensitivity to variation of the chain length in the polyamine backbone was further investigated by examining the ability of homoparabactin, norparabactin and parabactin to reverse EDDA induced iron starvation on agar plates, seeded with Paracoccus denitrificans. At extremely low ligand concentration (0.1 mmoles) parabactin and norparabactin were very efficient in their abilities to reverse iron-starvation induced by EDDA. In fact, at 90 h the diameter of bacterial growth in the presence of norparabactin was just 15% less than compared to parabactin. In contrast, there was no bacterial growth

detectable at 90 h in the presence of homoparabactin. As all three ligands would be expected to exist in the Λ-coordination isomer, the bacteria must use means in addition to chirality in the recognition of the ferric-siderophore complex. It is evident that the disposition of the spermidine backbone is one of those factors. While the symmetrical 3,3 backbone of norparabactin is recognized nearly as well as the natural siderophore by the _Paracoccus_ _denitrificans_ iron transport apparatus, the incorporation of one additional methylene unit into the spermidine backbone is apparently a significant enough change to render the complex unrecognizable to the membrane receptor or perhaps interferes with the next step in the processing of the ferric siderophore receptor complex.

CHAPTER III
SYNTHESIS AND CHARACTERIZATION OF A PARABACTIN
PHOTOAFFINITY LABEL

Introduction

Over the past few decades a great deal of research has been
amassed regarding microbial iron assimilation. In the 1950's came the
revelation that certain microbial natural products were functioning as
so called "iron carriers." Since that time a variety of these ferric
ion specific siderophores have been isolated and characterized. It is
now generally accepted that virtually all aerobic and facultative
anaerobic microbial species produce and/or utilize siderophores for the
sole purpose of solubilizing and sequestering iron to meet the metabol-
ic demands of the cell. While a number of siderophores have been
classified to date, it is safe to say that many more remain to be char-
acterized. Several intriguing mechanisms by which siderophores mediate
iron transport have been elucidated in both prokaryotic and eukaryotic
species. It is becoming more and more apparent that these iron uptake
mechanisms involve interactions between the siderophore iron complex
and specific surface receptors present in the cell. A logical progres-
sion which has followed over the past several years has been a shift to
research investigating the properties of the receptor proteins. A
recurring theme appears to be the induction of the membrane receptors
in conjunction with the synthesis of the siderophore in response to
iron deprivation.[52] The demonstration of the induction of bacterial
outer membrane proteins in vivo during infection may hold much promise

41

in the eventual production of vaccines specific for these proteins. While this potential avenue against infection is just now being recognized, it is obvious that much needs to be learned regarding the nature and composition of these proteins. Unfortunately, only in the case of E. coli has a siderophore receptor been purified and its physical characteristics elucidated.[79]

Our investigation into the mechanism of the parabactin mediated iron transport apparatus in Paracoccus denitrificans strongly suggests the presence of a membrane receptor responsible for the stereospecific binding of the ferric L-parabactin complex. It is with these results in mind that we have undertaken the isolation and characterization of the membrane receptor protein responsible for siderophore binding and iron removal in Paracoccus denitrificans. A potentially useful method to explore the interactions between the siderophore iron complex and the receptor protein is through the use of photoaffinity labeling. The photoaffinity label contains a photoreactive functionality which upon photolysis is capable of forming a covalent bond with the receptor protein. In this way a specific receptor protein can be selectively and irreversibly labeled to facilitate its isolation and eventual structural elucidation.

We have decided to examine the potential use of a photoaffinity label to identify the membrane receptor protein responsible for binding to the siderophore, parabactin. If successful, the properties of the receptor will be investigated, e.g. molecular weight and chromatographic behavior. It would then be possible to isolate the unlabeled receptor in order to characterize its physical and chemical properties.

The specific aims include the design and synthesis of a photoaffinity label and the experiments evaluating its effectiveness at substituting for parabactin at the receptor level. These include

1. A comparison of the conformation of the photoaffinity labels' gallium chelate with that of parabactin's gallium chelate utilizing 300 MHz ^{1}H NMR;

2. The evaluation of the photoaffinity label's ability to promote the growth of Paracoccus denitrificans under limited iron conditions; and

3. A comparison of the photoaffinity label's ability to promote iron incorporation into cell suspensions of Paracoccus denitrificans with that of parabactin utilizing both [^{55}Fe] and [^{3}H] labeled ligands.

Once having successfully shown that the photoaffinity label is recognized by the parabactin receptor and that it promotes iron incorporation into the cell in the same manner as parabactin, it will be possible to begin the actual labeling and isolation studies.

Experimental

General

Reagents were purchased from Aldrich Chemical Co. and used without further purification unless otherwise stated. The [^{55}Fe] ferric chloride, specific activity 43.6 Ci/g in 0.5 M hydrochloric acid and the Biofluor scintillation cocktail were purchased from New England Nuclear Corp. The [^{59}Fe] ferric chloride specific activity 11.5 mCi/mg in 1.0 N hydrochloric acid was purchased from ICN Biomedicals, Inc. Activated CH-Sepharose 4B and Sephadex LH-20 were purchased from

Pharmacia Fine Chemicals. Gallium (III) nitrate nonahydrate was pur-
chased from Alfa. Filters used in the transport assays were Gelman
GA-6 membrane filters and were 0.45 μm pore diameter. Trypticase soy
agar and trypticase soy broth were purchased from BBL Microbiology Sys-
tems. Proton NMR spectra were recorded on a Nicolet NT-300, 300 MHz
instrument or a Varian EM-390 90 MHz instrument. IR spectra were
recorded on a Beckman Acculab 1 Spectrophotometer. Elemental analyses
were performed by Atlantic Microlabs, Atlanta, GA, or Galbraith Labora-
tories, Knoxville, TN. Melting points were taken on a Fisher-Johns
apparatus and are uncorrected. Photolysis experiments were performed
using a Rayonet type RS photochemical reactor. Gallium chelates used
for high field NMR studies were prepared by first solubilizing the lig-
and in an aqueous methanol solution at pH 8.5. A slight excess of gal-
lium III nitrate was then added and the pH adjusted to 7.5. The reac-
tion mixture was allowed to stir for 1 h at which time excess solvent
was removed _in vacuo_. Tritium parabactin was prepared and purified in
a manner identical to parabactin starting with L-[^{3}H] threonine.
Final specific activity 1.05 x 10^7 DPM/mg.

Growth Studies

The effects of parabactin and parabactin azide on the growth of
Paracoccus denitrificans in iron-deficient media were determined.
Iron-free ligands (2 μM) were added in methanol to sterile Klett
flasks, evaporated to dryness under nitrogen which had been passed
through a 0.22 μ millipore filter and redissolved in sterile growth
media. The media was used as previously described.[19] Growth rates
were determined by monitoring Klett readings versus time. Standard

curves were generated correlating Klett units with colony forming units (CFU) using serial plating techniques. Growth studies were reported as CFU's versus time.

HPLC

HPLC was performed on a Rainin Rabbit 4P/4PX system utilizing a C-18 reverse phase column. The mobile phase contained 80% acetonitrile/20% 0.01 M ammonium phosphate buffer, pH 3.0. For preparative HPLC, the buffer was omitted from the aqueous phase.

Transport Assays

Individual colonies of _Paracoccus denitrificans_ were inoculated into 20 mL of trypticase soy broth and incubated for 24 h at 30°C with rotary shaking. Inoculations were then made into liquid culture medium at 20 µL of broth per 10 mL of culture media and incubated with rotary shaking at 30°C. Cells were harvested after 48 to 72 h by centrifugation at 5000 g for 20 minutes at 4°C, washed twice with cold culture medium and resuspended in fresh culture medium to a Klett reading of 150. Stock solutions of chelates including ^{55}Fe and ^{3}H labeled ferric parabactin and parabactin azide were added to the cell suspensions and incubated with rotary shaking at 30°C. At various time points, aliquots were removed (200 µL) and immediately diluted with cold culture medium (5 mL). This mixture was then rapidly filtered through a Gelman GA-6 membrane filter. The filters had been presoaked in a 1 mM unlabeled chelate solution to decrease adsorption of the labeled chelate to the filters and were rinsed once with culture medium (5 mL) before filtering the cell suspensions. After the cells had been collected, the filters were rinsed with cold culture medium (5 mL). Liquid scintilation counting of the air-dried filters was then performed in 10 mL

of Biofluor cocktail. Control values of labeled chelates adsorbed to the filters in the absence of cells were determined, then substracted from the values obtained with cells present. Uptake of labeled chelates by cell suspensions of Paracoccus denitrificans is presented as "percent uptake," which indicates the percentage of the total amount of added label that has been taken up by the cells.

Photolysis Experiments

Various concentrations of [Fe] or [H] labeled ferric parabactin azide were incubated with Paracoccus denitrificans membrane preparations in the dark for 30 min at room temperature. Samples were then placed in quartz tubes and photolyzed in the Rayonet photo-reactor for 5-10 min while rotating in a carousel. Protein was precipitated by addition of ammonium sulfate to 80% saturation. Samples (50 µg) were then subjected to SDS-gel electrophoresis as described by Laemmli. Autoradiography of the dried gel was performed by placing the gel in contact with Kodak X-Omat film and developed after 7 days. For detection of tritium label the gel was incubated with salicylate as described by Chamberlain[81] before drying.

2-Hydroxy-4-nitrobenzonitrile (1) was prepared from 2,4-dinitrophenylacetic acid as previously described.[82]

4-Amino-2-hydroxybenzonitrile·HCl (2). Compound 1 (2.10 g, 12.80 mmol) was dissolved in 200 mL of ethanol containing 5 mL of concentrated HCl. The reaction mixture was heated to reflux, at which point 3.0 g of iron powder was added in portions over a period of 3 h with continued heating. The reaction mixture was then cooled to room temperature. The ethanol was removed in vacuo and the residue was taken up in

water (150 mL) and extracted into ether (5 x 50 mL). The ether was dried and concentrated to afford the crude product. Further purification was effected by chromatography on silica gel, using 10% MeOH/CHCl$_3$ as eluant to afford 1.10 g (50%) of product: mp 184-185°C to afford 1.10 (50%) of product: mp 184-185°C (lit. 186°C).[83]

4-Azido-2-hydroxybenzonitrile (3). Compound (2) (0.90 g, 5.28 mmol) was suspended in 10 mL of ice-cold concentrated HCl. To this cooled solution NaNO$_2$ (0.65 g, 9.4 mmol) in 5 mL of water was added slowly with stirring over a period of 1 h. This was followed by addition of NaN$_3$ (0.60 g, 9.2 mmol) in 5 mL of water. The mixture was stirred for an additional 1 h; then the cooled reaction mixture was filtered and the residue washed with ice-cold water to yield 0.72 g of (3) in 85% yield. ^{1}H NMR (10:1 COCl$_3$/DMSO-d6) δ 6.58 (m,2H), 7.44 (d, 1H); IR (KBr), 3200 cm^{-1} (br), 2240 (s), 2110 (s), 1600 (s), 1480 (s), 1285 (s). m.p. 148-149°C.

2-Hydroxy-5-nitrobenzonitrile (8) was prepared utilizing published procedures.[84]

5-Amino-2-hydroxybenzonitrile·HCl (9) was prepared and purified analogously as (2) mp 160-162°C (lit. 162°C).[85]

5-Azido-2-hydroxybenzonitrile (10) was prepared and purified as described for compound (3): 82% yield; ^{1}H NMR (10:1 COCl$_3$/DMSO-d6) δ 7.03 (m, 2H), 7.11 (d, 1H); IR (KBr), 3200 (br), 2230 (s), 2100 (s), 1510 (s), 1260 (s).

Ethyl 2-hydroxy-4-nitrobenzimidate·HCl (5). Vacuum-dried 2-hydroxy-4-nitrobenzonitrile (1) (0.71 g, 4.33 mmol) was suspended in 10 mL dry absolute ethanol and dry HCl was bubbled through the cooled

mixture for 1 h. The reaction mixture was allowed to sit for 48 hr at room temperature at which point the product was recovered by filtration and dried under vacuum to afford 0.90 g (84%) of product. ^{1}H NMR (DMSO-d_6) δ 1.40-1.52 (t, 3H), 4.54-4.68 (q, 2H), 7.70-7.75 (d, 1H), 7.91-8.0 (d, 1H), 8.04-8.09 (s, 1H). m.p. 196-198°C Decomp. Anal. Calcd for $C_9H_{11}N_2O_4Cl$: C, 43.83; H, 4.49; N, 11.36. Found: C, 43.75; H, 4.52; N, 11.32.

  Ethyl 4-amino-2-hydroxybenzimidate·HCl (6). Ten percent palladium on carbon (0.99 g) was added to a solution of (5) (2.10 g, 8.51 mmol) in dry absolute ethanol (100 mL). The solution was stirred under a hydrogen atmosphere for 7 h. The solution was then filtered through a medium (10-15) frit and washed with ethanol. The solvent was evaporated and the residue was purified by chromatography on silica gel, using 10% MeOH/CHCl$_3$ as eluent to afford the product (6) in near quantitative yield. ^{1}H NMR (7:3 COCl$_3$:DMSO-d_6) δ 1.54 (t, 3H), 4.58 (q, 2H), 6.03 (br, 2H), 6.28 (d, 1H), 6.42 (s, 1H), 7.58 (d, 1H), 9.41-10.70 (m, 3H) m.p. 155-156°C.
Anal. Calcd for $C_9H_{13}N_2O_2Cl$: C, 49.89; H, 6.05; N, 12.93.
Found: C, 49.82; H, 6.08; N, 12.90.

  Ethyl 4-azido-2-hydroxybenzimidate·HCl (7). To a suspension of (6) (0.96 g, 4.43 mmol) in 100 mL of ethyl acetate was added freshly distilled isoamyl nitrite (714 μL, 5.32 mmol) and 75 μL of acetic acid. The mixture was cooled and stirred for 3 h at which time (0.35 g, 5.38 mmol) of NaN$_3$ was added. After an additional 3 h the reaction mixture that resulted was filtered and washed with ethyl acetate. The solvent was removed, and the residue was purified by chromatography on

silica gel using 10% MeOH/CHCl$_3$, as the eluent to afford (0.25 g) product. ^{1}H NMR (DMSO-d$_6$) δ 1.49 (t, 3H), 4.13 (q, 2H), 6.48 (d, 1H), 6.64 (s, 1H), 7.75 (d, 1H); IR (KBr), 3020 (br), 2090 (s), 1595 (br), 1510 (br), 1260 (br), 1085 (br).

Nitro parabactin (8). Vacuum dried ethyl 2-hydroxy-4-nitrobenz-imidate (5) (0.25 g, 1.19 mmol) and bis N^1,N^8-2,3-dihydroxybenzoyl)-N^4-(L-threonyl)spermidine·HBr^{28} (I) (0.59 g, 0.98 mmol) were heated at reflux in dry, degassed methanol (50 mL) for 20 h. The solution was cooled and concentrated. The residue was dissolved in ethanol and dry packed on Sephadex LH-20. Column chromatography of the residue on LH-20, using 20% EtOH/benzene as the eluent, afforded 0.55 g (85%) of product. ^{1}H NMR (10:1 CDCl$_3$/DMSO-d$_6$) δ 1.35-1.51 (2d, 3H), 1.51-2.01 (m, 6H), 3.18-3.72 (m, 8H), 4.58-4.63 (2d, 1H), 5.31-5.48 (m, 1H), 6.50-6.65 (M, 2H); 6.81-6.91 (m, 2H), 7.01-7.15 (m, 2H), 7.58-7.77 (m, 3H), 7.81-8.15 (m, 2H); mass spectrum m/e 666 (M + 1).

Anal. Calcd. for C$_{32}$H$_{35}$N$_5$O$_{11}$ 0.5 H$_2$O: C, 56.97; H, 5.38; N, 10.38. Found: C, 57.02; H, 5.38; N, 10.32

Amino parabactin (9). Ten percent palladium on carbon (0.24 g) was added to a solution of (8) (0.54 g, 0.80 mmol) in dry absolute eth-anol (75 mL). The solution was stirred under a hydrogen atmosphere for 6 h. The suspension was then filtered through a medium (10-15) frit and the residue was washed with ethanol. Concentration of the filtrate was followed by purification of the residue on Sephadex LH-20, using 20% EtOH in benzene as the eluent to afford 0.45 g (89%) of product. ^{1}H NMR (10:1 CDCl$_3$/DMSO-d$_6$) δ 1.35-1.51 (2d, 3H), 1.55-2.10 (m, 6H), 3.20-3.71 (m, 8H), 4.47-4.66 (2d, 1H), 4.70-5.01 (m, 2H), 7.16-7.31 (m

2H), 7.33-7.46 (m, 1H), 8.05-8.41 (m, 4H); mass spectrum, m/e 636

(M + 1).

Anal. Calcd for $C_{32}H_{37}N_5O_8$: C, 60.46; H, 5.87; N, 11.02.

Found: C, 60.45; H, 5.83; N, 11.05.

Parabactin Azide (10). Vacuum-dried ethyl 4-azido-2-hydroxy-

benzimidate (7) (0.13 g, 0.63 mmol) and bis N^1,N^8-(2,3-dihydroxy-

benzoyl)-N^4-(L-threonyl)spermidine·HBr (I) (0.30 g, 0.50 mmol) were

heated in dry degassed refluxing methanol (50 mL) for 20 h. The solu-

tion was concentrated and the residue was dissolved in ethanol then dry

packed on Sephadex LH-20. Column chromatography on LH-20, using 15%

EtOH in benzene as eluent afforded 0.25 g (76%) of product. ^1H NMR

(10:1 $CDCl_3/DMSO-d_6$) δ 1.41-1.56 (2d, 3H), 1.55-2.10 (m, 6H),3.21-3.71

(m, 8H), 4.60-4.71 (2d, 1H), 5.35-5.49 (m, 1H), 6.52-6.73 (m, 4H), 6.96

(d, 2H), 7.17 (t, 2H), 7.63 (t, 1H), 8.02-8.26 (m, 2H); IR (KBr), 3350

(br), 2110 (s), 1640 (s), 1265 (s) cm^{-1}; mass spectrum, m/e 661 (M + 1)

Parabactin Coupled Resin. Dry activated CH-Sepharose 4B resin

(Pharmacia Fine Chemicals, Uppsala, Sweden) was swelled in 10^{-3} M HCl

(50 mL) for 30 min. The swelled resin was rinsed in 0.1 M HEPES buffer

(N-2-Hydroxyethylpiperazine-N'-2-ethanesulfonic acid) pH = 7.5.

A solution of amino parabactin (67 mg) dissolved in coupling

buffer containing methanol (4 mL) and 0.1 M HEPES buffer pH = 7.5 (2

mL) was added to 3 mL of the swelled CH-Sepharose 4B resin in a sealed

glass tube under an argon atmosphere. The tubes were rotated at 12 rpm

for 24 h. The resin was then filtered and exhaustively washed with

coupling buffer. Unreacted N-hydroxysuccinimide ester groups on the

resin were then deactivated by addition of 1 M ethanolamine HCl (0.1 mL/mL gel) pH = 8 for 30 min. The resin was washed with 3 cycles of alternative 0.1 M TRIS-HCl buffer pH = 8 (50 mL) and 0.1 M Na acetate buffer pH = 4 (50 mL). A control resin was subjected to identical coupling conditions as above, however parabactin was added in place of amino parabactin.

To a dilute solution of methanolic $FeCl_3$ (1 mg/mL) was added 250 µL of $^{59}FeCl_3$ (100,000 counts/100 µL). To 1.0 mL of resin was added 500 µL of the radioactive iron solution and the mixture rotated for 12 h. The purple resin that resulted was first washed with coupling buffer (3 x 3 mL) then suspended in a 10 µM EDTA solution (3 mL) and rotated for 30 min. The EDTA washings were continued until counts on the control resin which had been reacted with parabactin were negligible. In order to determine coupling efficiency, the amount of iron bound to the amino parabactin coupled resin was measured. Sample radiation of the resin was counted with an automatic gamma counter (LKB-Wilac Ria Gamma 1274, Wallac Oy, Finland) and indicated 20% coupling efficiency.

All spectral data are in the Appendix.

Results

Design and Synthesis of a Parabactin Photoaffinity Label

There are a number of ways one can consider activating parabactin so that it will covalently and irreversibly bind to its bacterial receptor, e.g. introduction of masked nitrenes, alkylating or acylating functionalities in the ligand. As we do not know anything about

the nature of the parabactin receptor, a fairly active nonfunctionally selective device is required. The reagents selectivity must be in its ability to bind largely to its own receptor and react with it. In keeping with the synthetic problems and the required reactivity of the receptor label, we have chosen to consider parabactin azides A + B (Fig. 3-1). The azide on photolysis will produce an active nitrene capable of forming a covalent bond with the receptor protein. Furthermore, the use of nitrenes generated photochemically from azides to label isolated proteins or even cell associated systems is well documented.[86-88]

The design and synthesis of the receptor label will of course be predicated on parabactin. The molecule will ultimately contain a tritium label. The boundary conditions we have set for this ligand in terms of its required behavior are: (1) It must bind iron similarly to parabactin. (2) It should promote uptake of iron by the microorganism. (3) It must be accessible synthetically in moderate quantities.

The question of course arises as to precisely where to introduce the azide functionality in the parabactin molecule. Clearly, it must be introduced at a position which will not inhibit iron chelation, receptor association, or iron transfer into the cell. It is clear from CPK models that we cannot put the azide next to the hydroxyl on the central aromatic ring because it is quite possible that this will induce a different mode of ligand metal binding. This then limits us to introducing the azide functionality para or meta to the
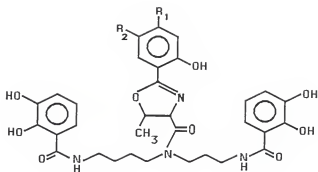
Figure 3-1. Structures of parabactin azide. (a) R_1 = N_3, R_2 = H and (b) R_1 = H, R_2 = N_3.

hydroxyl on parabactin's central aromatic ring (Figs. 3-2, 3-3). In these systems the photoaffinity functionality should be far enough removed from the ligand's chelating groups so as not to alter their metal binding properties. The decision to place the azide functionality on the central aromatic ring as opposed to the terminal rings, was based on the fact that the last step in the synthesis of parabactin involves fixing of the central aromatic piece to N^1,N^8-bis-(2,3-dihydroxybenzoyl)-N^4-threonyl spermidine (I).[28] In this way the azide functionality does not have to sustain any unwanted reaction conditions involved in the synthesis of (I).

There is considerable precedent in the literature for the synthesis of aryl azide imidates in high yield using the commercially available 4-aminobenzonitrile.[89,90] In a model experiment designed to evaluate the stability of an aromatic azide fixed to an oxazoline ring, we synthesized ethyl 4-azidobenzimidate[89] and successfully condensed it with the parabactin precursor (I) to yield the corresponding parabactin analogue (Fig. 3-4) (mass spectrum m/e 646). The compound proved to be stable in the dark and easily isolable by chromatography on Sephadex LH-20. The stability of the azide imidate to the condensation reaction conditions and its ease of synthesis did not suggest there would be any problems in generating ethyl 4-azido-2-hydroxybenzimidate. However, this was not the case.

As the last step in the synthesis of parabactin involves coupling of ethyl 2-hydroxybenzimidate with (I) it is clear that this imidate represents the optimum target for fixation of the azide

Figure 3-2. CPK model of the gallium (III) chelate of parabactin azide A.

Figure 3-3. CPK model of the gallium (III) chelate of parabactin azide B.
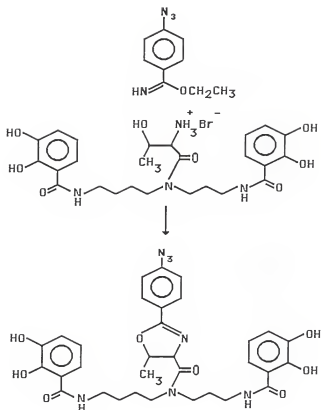
Figure 3-4. Synthesis of deoxyparabactin azide.

functionality. The standard protocol for the synthesis of aryl azide imidates involves the initial conversion of a nitro aryl nitrile to the corresponding amino aryl nitrile followed by conversion of the amino function to the azide. The production of an azide generally involves reaction of the amine in concentrated acid with aqueous sodium nitrite followed by the addition of sodium azide. The intermediate diazonium compound is generally not isolated. This kind of synthesis was attempted with 2-hydroxy-4-nitrobenzonitrile (1) (Fig. 3-5). The nitro group was first reduced to the corresponding amine (2) utilizing iron and hydrochloric acid which proceeded in 50% yield. Treatment of (2) with aqueous sodium nitrite in concentrated hydrochloric acid followed by exposure of the diazonium compound to sodium azide resulted in (3) in 80% yield. Unfortunately, we were unable to convert (3) to the imidate (4) by treatment with anhydrous ethanolic hydrochloric acid even in a variety of solvents. A similar sequence was effected on 2-hydroxy-5-nitrobenzonitrile (8) (Fig. 3-6). Again the amino compound (9) was obtained in 50% yield and conversion of this to the azide (10) proceeded in 80% yield. However, attempted conversion of this azide to the imidate (11) by treatment with ethanolic hydrochloric acid, again in a variety of solvents resulted in the amine (12). This collapse of the azide (10) to the amine under acid conditions can probably be attributed to the para relationship of the azide functionality to the phenolic hydroxyl. This instability suggests that ethyl 5-azido-2-hydroxybenzimidate might not be a suitable intermediate in the synthesis of
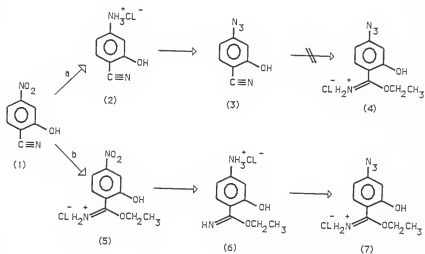
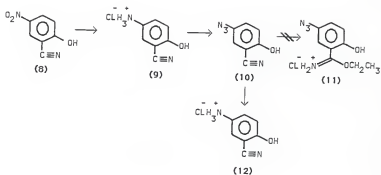Figure 3-5. Synthesis of parabactin azide A precursor.

Figure 3-6. Synthesis of parabactin azide B precursor.

parabactin azide. Consequently, the alternative path (b) (Fig. 3-5)
was considered. The nitrile (1) was converted to the nitroimidate
(5) in 80% yield by treatment with anhydrous ethanolic hydrochloric
acid. We next determined that the nitro group in imidate (5) could
be reduced to the corresponding amine quantitatively by hydrogenation
over palladium. Fortunately the imidate was left intact and the
compound did not polymerize. Next the imidate (6) was taken to the
azide (7) in 30% yield by treatment with isoamyl nitrite and acetic
acid in ethyl acetate followed by exposure to sodium azide. The low
yield is probably associated with the hydrochloride's poor solubility
in ethyl acetate. Finally, ethyl 4-azido-2-hydroxy benzimidate (7)
(Fig. 3-5) was allowed to react with bis $N^1,N^8(2,3$-dihydroxybenz-
oyl)-N^4-threonyl spermidine hydrobromide in refluxing methanol to
produce parabactin azide (Fig. 3-7) in 76% isolated yield.

All reactions after production of the amino compounds (2) and
(6) (Fig. 3-5) and (9) (Fig. 3-6) were carried out in minimal light.
The azide of interest, ethyl 2-hydroxy-4-azidobenzimidate when run on
TLC and exposed even briefly to a UV lamp for identification, quickly
turned yellow. Parabactin azide itself must also be handled
cautiously with regards to light exposure.

Proof of Structure

Several lines of evidence were utilized as proof of structure
for the azide. It is important to point out that because of the
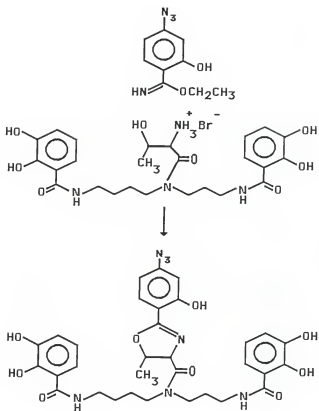compounds thermal and light sensitivity elemental analysis was

Figure 3-7. Synthesis of parabactin azide A.

unobtainable. The azide inevitably decomposed in the hands of the analytical companies. A comparison of the 300 MHz ^{1}H NMR of parabactin and parabactin azide reveals the two compounds to be essentially identical, including duplicity of signals due to hindered rotation about the central amide bond. However, as expected, the aromatic region was different.

In order to assign the aromatic ring protons of the azide to specific ^{1}H NMR signals, we found it practical to compare the 300 MHz ^{1}H NMR of the parabactin and parabactin azide gallium complexes. In the spectra of the parabactin gallium (III) chelate, the proton meta to the hydroxyl in the central aromatic ring is found to be a triplet centered at 7.21 ppm (Fig. 3-8). However, in the spectra of the parabactin azide gallium (III) complex, the signal at 7.21 ppm is absent (Fig. 3-9). These spectra indicate that the compound at hand is a parabactin derivative substituted on the central aromatic ring meta to the hydroxyl. The infrared spectrum of parabactin azide run as a KBr pellet shows the characteristic absorption at 2110 cm^{-1} for N_3. Unfortunately, the signal for the diazonium functionality of the synthetic precursor can also occur at essentially the same wavelength.

Additional proof of structure was obtained from the pyrolysis and photolysis of parabactin azide (Fig. 3-10). The thermal decomposition of parabactin azide was carried out in boiling tetralin at 207°. This resulted in a number of decomposition products including amino parabactin (the synthesis of which is described below). This arises from first loss of nitrogen leading to the unstable nitrene,

	# H's
a- 7.42 d	1
b- 7.21 t	1
c- 6.84 t	1
d- 6.76 d	1
e- 6.66 t	1
f- 5.42 t	1
g- 6.35 d	1
t- 6.16 m	2
i- 6.07 t	1

a coupled to f   f--> doublet

b coupled to e+f [e--> singlet / f--> doublet]

c coupled to t

d coupled to i   i--> doublet

e coupled to b   b--> doublet

f coupled to a+b

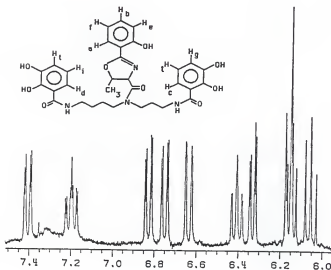g coupled to t

t coupled to c,g,i

i coupled to d+t

Figure 3-8. Chemical shift and coupling data for the aromatic ring protons of the parabactin gallium (III) chelate in d_6-DMSO.
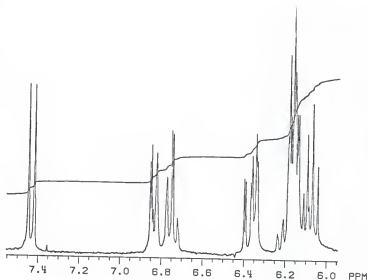
Figure 3-9. 300-MHz ^{1}H NMR spectrum of the aromatic ring protons of the parabactin azide gallium (III) chelate in d$_6$-DMSO.
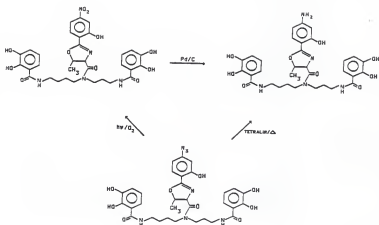
Figure 3-10. Structures of the reaction products isolated from the pyrolysis and photolysis of parabactin azide.

which then abstracts hydrogen from the solvent.[91] The product had an RF on silica gel identical with synthetic amino parabactin and the same retention time on HPLC.

The photochemical decomposition of aromatic azides in the presence of oxygen has recently been investigated.[92,93] One of the products, the corresponding nitro derivative was shown to be formed by the trapping of triplet aryl nitrenes by triplet oxygen. With the successful synthesis of nitro parabactin (see below), the photochemistry of parabactin azide in the presence of oxygen could be evaluated. The initial photolysis experiments were run using dilute solutions (10^{-4} M) of parabactin azide in acetonitrile or benzene under a steady stream of oxygen. Unfortunately, this resulted in the formation of intractable tars and complete decomposition of the azide as detected by HPLC. However, on a change of the solvent to acetone, the azide was extremely stable and after photolysis for 24 h under a stream of oxygen, several products were detected by HPLC. Indeed, a major product had an identical retention time as synthetic nitro parabactin, however, attempts at distinguishing this from parabactin failed. The photodecomposition product was therefore isolated using preparative HPLC. The isolated compound was then subjected to high field NMR and the aromatic region compared to both synthetic nitro parabactin and parabactin. Utilizing ^{1}H NMR difference spectroscopy it was shown that the photodecomposition product was identical to nitro parabactin indicating that indeed the nitrene was capable of inserting into oxygen.

Finally, the most significant proof of structure was obtained using fast atom bombardment (FAB) mass spectroscopy. A mass peak at 661 was observed corresponding to the intact azide along with a peak at 635, arising from loss of molecular nitrogen and proton abstraction, corresponding to amino parabactin. It should be noted that attempts at simple CI and EI mass spectroscopy were unsuccessful in observing a molecular ion. We regard the accumulated evidence as proof of structure for parabactin azide. The synthesis has since been repeated using tritiated threonine in the synthetic scheme thus providing parabactin azide with a completely tritiated oxazoline ring. The specific activity was determined to be 10.5×10^6 DPM/mg.

The ease of access and stability of the nitro imidate (5) (Fig. 3-5) encouraged us to generate amino parabactin for use in the production of a parabactin affinity chromatography column. The nitro imidate (5) was condensed with the parabactin backbone (1) in refluxing methanol to afford nitro parabactin in 85% yield. The nitro functionality was then reduced to the corresponding amino compound by hydrogenation over palladium to afford amino parabactin (Fig. 3-11). Amino parabactin was then reacted with activated CH-Sepharose 4B, in aqueous methanol-HEPES buffer to produce the first polyamine siderophore affinity column.

Activated CH-Sepharose 4B is produced by the esterification of the carboxyl group of CH-Sepharose 4B using N-hydroxysuccinimide. The N-hydroxysuccinimide active ester is highly reactive with primary amino groups. Upon addition of ligand the N-hydroxysuccinimide group is displaced and a stable amide bond is formed. Since activated
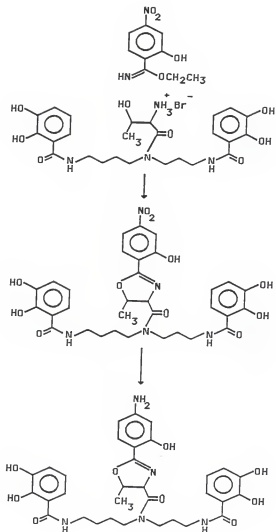
Figure 3-11. Synthesis of nitroparabactin and aminopara-
bactin.

CH-Sepharose 4B is specific for primary amino groups other active groups present in the ligand do not need to be protected prior to coupling. The reaction was run for 24 h at room temperature and the resulting matrix washed exhaustively with coupling buffer. The washing was continued until the eluant was negative to ferric chloride. A radioactive assay employing $^{59}FeCl_3$ was used to determine the amount of ligand coupled to the resin. Gamma counting of the $^{59}Fe^{+3}$ chelated to the ligand, which binds in a 1:1 stoichiometry, indicates a 20% coupling efficiency of amino parabactin with the resin.

Growth Stimulation and Uptake Characteristics of Parabactin Azide

The key issue in the design of a parabactin photoaffinity label is that it be recognized by the <u>Paracoccus denitrificans</u> parabactin receptor. The simplest way to ascertain whether or not the modified parabactin is utilized by this receptor is simply to measure its ability to stimulate the microorganism's growth in a low iron environment. Consequently, both parabactin and parabactin azide were compared in their ability to stimulate the growth of <u>Paracoccus denitrificans</u> in a minimal iron media (Fig. 3-12). As is clear from this figure, both parabactin and parabactin azide stimulate microbial growth to essentially the same degree. To further substantiate that parabactin azide behaves biologically like parabactin, a closer examination into its mechanism of iron-transport was required. It has been demonstrated that parabactin supplies iron to <u>Paracoccus</u>
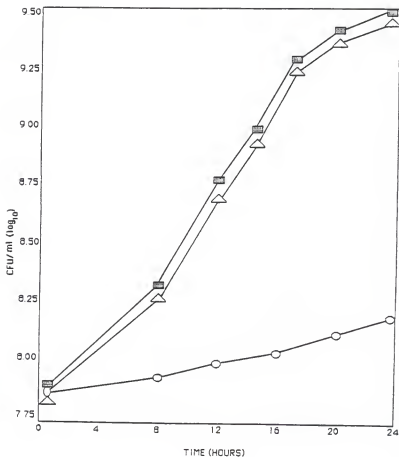
Figure 3-12. Growth rate of <u>Paracoccus denitrificans</u> in the presence of parabactin (■) (2 μM), parabactin azide (△) (2 μM), or controls (O).

denitrificans via an "iron-taxi" mechanism in which only the metal is incorporated into the cells. We have compared the ability of para-bactin azide to promote [^{55}Fe] incorporation into the micro-organism with that of parabactin.

Cell suspensions of Paracoccus denitrificans in late log phase, grown under iron deficient conditions, were tested for their ability to transport 1 μM [^{55}Fe] ferric parabactin azide and [^{55}Fe] ferric parabactin. The data indicate that both parabactin and parabactin azide promote iron uptake to essentially the same degree. There is a fairly rapid incorporation of the [^{55}Fe] label into the cells during the first 10 min of the experiment, followed by a steady increase until the iron uptake begins to level off at about 35% of the total label taken up after 45 min (Fig. 3-13). In the proposed "iron-taxi" mechanism of iron transport in Paracoccus denitrificans there is no appreciable transport of tritium labeled ferric L-parabactin. The ligand experiences only a transient association with a membrane receptor and remains extracellular. In order to monitor the fate of ligand in the ferric parabactin azide complex, cell suspensions were presented with the [^{3}H] ferric parabactin azide complex. As demonstrated in Figure 3-14 there is no appreciable transport of tritium labeled ligand (<10%) into the cell. There was observed an initial 4% cell-associated label after the first 5 min of the experiment which remained fairly constant over the remainder of the experiment. As expected, there was a steady uptake of the [^{55}Fe] labeled parabactin azide over the course of this experiment. Therefore it is apparent that in the dark parabactin

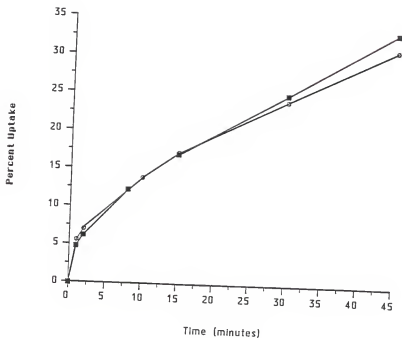Figure 3-13. Uptake of [^{55}Fe] ferric parabactin (■), and [^{55}Fe] ferric parabactin azide (O) by _Paracoccus denitrificans_.
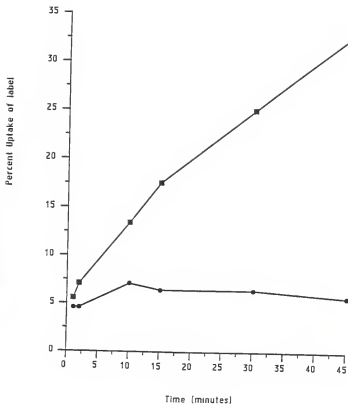
Figure 3-14. Uptake of [^{55}Fe] ferric parabactin azide (■), and [^{3}H] ferric parabactin azide (●) by <u>Paracoccus</u> <u>denitrificans</u>.

azide promotes iron incorporation into the cell in the same manner as parabactin i.e., via the "iron-taxi" mechanism. It was also important to demonstrate that parabactin azide was substituting for parabactin at the parabactin receptor site. An experiment designed to evaluate the effectiveness of parabactin azide at competing with parabactin for the receptor site was performed. Cells were presented with 10 μM [^{55}Fe]-ferric parabactin and various concentrations of nonradiolabeled ferric parabactin azide. The cells were incubated in the dark with rotary shaking at 30°C for 5 min, then assayed for uptake of radiolabeled iron. The data (Fig. 3-15) fit the curve predicted by simple competitive displacement of radiolabeled ferric parabactin by nonlabeled ferric parabactin azide in a ligand-receptor binding model[94] with properties analogous to Michaelis-Menten enzyme kinetics,[94] with a K_I = 2 μM. It should be mentioned that in this experiment the percent uptake of radiolabel in the absence of unlabeled parabactin azide was adjusted to 100% uptake. Additional values in the presence of nonradiolabeled parabactin azide were then normalized.

Photolabeling Studies

As an initial study, the photoreactivity of parabactin azide was determined utilizing UV spectroscopy. Spectra of a 10 μM sample of parabactin azide in culture media were obtained after repeated exposures to ultraviolet light. A Rayonet type RS photochemical reactor fitted with six 350 nm UV lamps was used as a light source. The spectra showed an absorption peak at 282 nm, corresponding to the azide functionality. This peak was gradually reduced upon photolysis
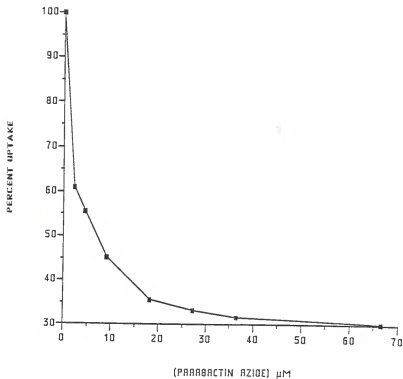
Figure 3-15. Competitive inhibition of [^{55}Fe] ferric parabactin uptake (■) by nonradiolabeled ferric parabactin azide in the dark. Incubation time: 5 min.

until its complete disappearance after illumination for a total of four min.

The choice of the proper wavelength for irradiation is an important consideration in photoaffinity labeling. Although irradiation with 254 and 300 nm lamps was very efficient in decomposing the azide functionality, irradiation at these shorter wavelengths was found to be very deleterious to the bacteria as determined from regrowth experiments. Therefore, we have chosen the longer wavelength of 350 nm which will photolyze the azide but have less adverse effects on the bacteria.

The following experiment was designed to evaluate the effects of photolysis on ferric-parabactin azide mediated iron uptake. It was first necessary to determine whether photolysis alone had any adverse effects on iron-uptake in cell suspensions of Paracoccus denitrificans. Cells, grown in iron deficient media, were harvested in late log phase. The resuspended cells were then placed in quartz tubes and photolyzed for 5 min while rotating in a carousel which held them 8 cm from the lamps. Cells were then assayed for $[^{55}Fe]$ ferric-parabactin uptake at 1.0 μM ferric chelate. A control experiment without irradiation was run consecutively. The data indicate that photolysis of cells alone resulted in approximatly 50% inhibition of iron uptake during the first 10 min of the experiment as compared to cells with photolysis (Fig. 3-16). The photolyzed cells were then able to gradually recover until the percent iron uptake was nearly identical to unphotolyzed cells after 75 min (data not shown). As a consequence, in an experiment involving photolysis of ferric-parabactin azide, photolyzed cells in the presence of ferric parabactin were used as controls.
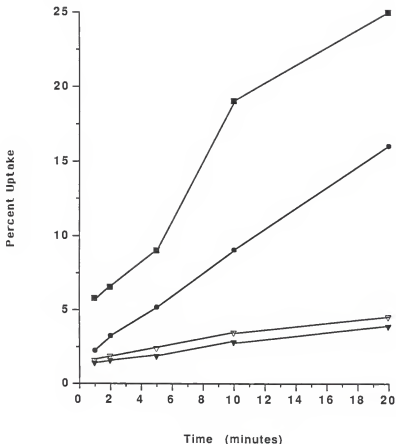
Figure 3-16. Effects of photolysis on [^{55}Fe] ferric parabactin uptake by a _Paracoccus denitrificans_.

Uptake of [^{55}Fe] ferric parabactin by untreated cells [■] or by cells which had been photolyzed prior to addition of radiolabel [●].

Uptake of [^{55}Fe] ferric parabactin by cells which had been incubated with 30 µM nonradiolabeled ferric parabactin [▽] or ferric parabactin azide [▼] and photolyzed prior to addition of radiolabel.

Photolysis of cells in the presence of ferric parabactin azide would be expected to irreversibly inhibit iron uptake by binding covalently at the ferric-parabactin receptor site and preventing further iron uptake. In order to assay for irreversible inhibition, cell suspensions were incubated with nonradiolabeled ferric-parabactin azide at 30 μM and irradiated for 5 min. The cells were then centrifuged and washed twice with ice-cold culture media to remove any unbound ligand. Resuspended cells, preincubated with shaking at 30°, were then assayed for iron-uptake with 1 μM [^{55}Fe]-ferric parabactin. The data (Fig. 3-16) show that photolysis of cells in the presence of ferric parabactin azide resulted in a slight inhibition of iron-uptake as compared to photolysis in the presence of ferric parabactin (10-15%).

The main objective in synthesizing the parabactin azide photoaffinity label was to identify the receptor protein responsible for siderophore binding in Paracoccus denitrificans in order to facilitate its eventual isolation. Experiments performed along these lines have involved the photolysis of parabactin azide in the presence of Paracoccus denitrificans membrane components. Samples were then subjected to gel electrophoresis and incorporation of radiolabel assessed by autoradiography of dried gels. Initial photolysis experiments were performed utilizing [^{3}H] labeled ferric parabactin azide. When whole membranes were photolyzed in the presence of the tritium labeled ligand there was no incorporation of radiolabel observed into any of the protein bands as detected by autoradiography. It was assumed that the low specific activity of the tritium labeled parabactin azide coupled to the inherent difficulties in detecting the

low energy beta particles were the causes. To circumvent these draw-
backs the [^{55}Fe] ferric chelate of parabactin azide with a high
specific activity was employed. This has the added benefit of facil-
itating detection without the need for pretreatment of the gel with a
scintilation fluor. To demonstrate the ability of [^{55}Fe] labeled
ferric parabactin azide to label the parabactin receptor site, photo-
lysis was performed in the presence of a high concentration of photo-
affinity label (20 μM). In this way the specific activity in the
reaction mixture (200 μl) was increased substantially to 4.0x10^7
DPM/100 μl. The autoradiograph (Fig. 3-17) demonstrates an undesir-
able degree of nonselectivity under these reaction conditions. Quan-
titation of labeled protein by fractionalization and solubilization
of individual gel slices followed by scintilation counting also
indicated a low efficiency of incorporated radiolabel. In order to
increase the photoaffinity labels ability to selectively label the
parabactin receptor protein the concentration of ligand was reduced
substantially. Figure 3-18 shows the results from one such experi-
ment where the concentration of parabactin azide was 0.5 μM (Lane 1)
and 2.0 μM (Lane 2). While in no way definitive, the autoradiograph
demonstrates an increase in selectivity when photolysis was performed
at low ligand concentrations. The association of radiolabel with the
low iron inducible high molecular weight proteins is evident. It is
noteworthy that these same protein bands appeared very intense when
photolysis was carried out at the higher ligand concentration.

Figure 3-17. Incorporation of radiolabel into <u>Paracoccus</u> <u>deni</u>-<u>trificans</u>' membrane preparations which had been incubated with 20 µM [^{55}Fe] ferric parabactin azide and photolyzed for 5 min.

Figure 3-18. Incorporation of radiolabel into _Paracoccus deni-trificans_' membrane preparations which had been incubated with 0.5 µM (Lane 1) and 2.0 µM (Lane 2) [^{55}Fe] ferric parabactin azide and photolyzed for 5 min.

Discussion

The use of photoaffinity labeling has many advantages over traditional affinity labeling methods. Affinity labeling typically involves modified ligands containing alkylating or acylating groups which are capable of reacting with various nucleophilic species. Thus the presence of amino acids at the binding site of the target macromolecule is necessary for the potential formation of a covalent bond with the affinity label. Photoaffinity analogues generate reactive intermediates upon photolysis i.e., nitrenes or carbenes which are capable of insertion into nucleophilic centers and of addition to double bonds and aromatic systems present in the macromolecule.[95,96] As the photo-generated species has a short half life (10^{-3} sec), label generated away from the active site would be expected to react preferentially with solvent before migrating to a nonspecific site. The photoaffinity label has the added advantage in that it is chemically inert in the dark. In this way the photoaffinity label's binding characteristics may be determined compared to the natural substrate. An examination of these reversible binding constants is extremely useful in designing photolabeling experiments. Nonspecific photolabeling caused by nonspecific reversible binding of the photoaffinity label is the most significant undesirable occurrence in photolabeling studies.[97] By determining the amount of reagent needed to saturate the receptor sites one can optimize the efficiency of site-specific photoaffinity labeling. Utilizing ligand concentrations much above this concentration would very likely result in increased nonspecific binding.

The results suggested that the parabactin photoaffinity label would be an effective means by which to identify the membrane receptor protein responsible for siderophore binding in Paracoccus denitrificans. It was demonstrated that parabactin azide formed a gallium (III) complex identical with the parabactin gallium (III) complex as determined by 300 MHz ^{1}H NMR. Furthermore, parabactin azide was shown to facilitate the growth of the microorganism as effectively as parabactin under the low-iron conditions present in the liquid culture medium. One might argue that parabactin azide was supplying iron to the cells by some other mechanism. While this appeared unlikely, it was nevertheless necessary to examine the mechanism of iron-uptake mediated by parabactin azide. When cells were presented with [^{55}Fe] labeled ferric parabactin azide, there was observed a rapid incorporation of radiolabel. The rate of uptake was identical to the rate observed in the presence of [^{55}Fe] labeled ferric parabactin. To monitor the fate of ligand, tritium labeled ferric parabactin azide was presented to the cells. As observed for parabactin there was no appreciable uptake of the tritium labeled ferric parabactin azide. These results demonstrated that parabactin azide was delivering iron to the microorganism in a manner identical to parabactin via an "iron-taxi" delivery system. The evidence also indicates that parabactin azide is able to compete effectively with parabactin for the parabactin receptor site in the absence of light. Increasing concentrations of nonradiolabeled ferric parabactin azide resulted in a steady decrease in the percent uptake of radiolabel from 10 μM [^{55}Fe] ferric parabactin with an approximate inhibitory concentration, K_I, in the range of 2-5 μM.

Initial experiments demonstrated that parabactin azide was, as expected, sensitive to irradiation. An absorption peak at 282 nm, corresponding to the azide functionality, was shown to disappear upon illumination. The photoreactive azide group upon photolysis decomposes to form a reactive but short-lived nitrene species. The aryl nitrene generated can occur in two electronic states, the singlet containing paired electrons or the triplet containing unpaired electrons. Triplet nitrenes typically abstract hydrogen with radical formation whereas singlet nitrenes are capable of inserting into the active site of the receptor protein.[96] The photolysis and pyrolysis experiments involving parabactin azide show that the ligand is capable of undergoing insertion reactions. If the nitrene generated by the photolysis of parabactin azide was efficiently binding to the parabactin receptor site one would expect to irreversibly inhibit iron uptake by the microorganism. When cell suspensions of Paracoccus denitrificans were photolyzed in the presence of ferric parabactin azide there was observed a small degree of inhibition of iron-uptake as compared to photolysis in the presence of ferric parabactin. Due to variation in iron-uptake from one experiment to another the significance of the datawas not determined. A closer examination of the data in Figure 3-16 reveals that photolysis of cells in the presence of parabactin or parabactin azide results in significant inhibition of iron-uptake as compared to cells photolyzed in the absence of ligand. After 20 min into the transport assay there is a four-fold decrease in iron-uptake by cells which were photolyzed in the presence of parabactin or parabactin azide. One explanation for

this observed behavior is that we simply have saturated the cells with iron when photolysis was performed in the presence of 30 μM unlabeled ferric siderophore. However, this requires that a regulatory mechanism exists by which the iron-uptake apparatus can be rapidly shut down at the first sign of high iron conditions. In this assay, the cells are presented with the ferric siderophore for 5 min during photolysis after which the cells are rapidly centrifuged and washed twice with cold buffer to remove excess ligand. As the entire washing procedure is complete in just a few minutes, we do not feel that this brief exposure to a high concentration of ferric siderophore can adequately account for the dramatic inhibition of iron-uptake. Another plausible explanation which is consistent with the results is that parabactin itself is acting as a photoaffinity label. This would certainly explain why there was only a slight inhibition of iron-uptake in the presence of parabactin azide as compared to controls containing parabactin. In order to justify such a hypothesis it would be necessary to demonstrate that parabactin undergoes some structural changes as a result of U.V. irradiation. A solution of parabactin (20 μM) in liquid culture media was photolyzed in a quartz cuvette for several min utilizing six 3000 Å U.V. lamps. The U.V. spectrum of the photolysis mixture revealed significant perturbations at 284 and 252 nm which increased with longer photolysis time. While these results are preliminary they do suggest that the observed inhibition of iron-uptake during photolysis in the presence of parabactin may be a consequence of its photo-reactivity. This will require further evidence such as the isolation and characterization of a photo-decomposition product. Another experiment which

may be very informative would involve photolysis of membrane preparations in the presence of [^{55}Fe] ferric L-parabactin. An autoradiographic analysis of the separated proteins demonstrating incorporation of radiolabel into protein bands would be direct evidence implicating parabactin as a photoaffinity probe.

Photolysis experiments designed to identify the parabactin receptor protein have for the most part been inconclusive. The major setback has been a lack of selectivity in the binding of the label to membrane preparations. Figure 3-17 demonstrates the lack of selectivity at high ligand concentration where it appears that increased labeling is proportional to increased protein concentration. At lower ligand concentrations the selectivity was increased (Fig. 3-18). A protein band in the 80,000 molecular weight range was more intense than other labeled bands as detected by autoradiography. This high molecular weight protein is not the most concentrated protein in the membrane preparations. While a definitive statement cannot be made, it is interesting to speculate on the role of these proteins in siderophore-mediated iron-uptake. The possibility exists that these proteins are subunits of the same receptor protein and that the observed binding to each is representative of the physiological function of the receptor protein.

In other photoaffinity systems scavengers have been employed to decrease nonspecific photolabeling.[98] These protective compounds prevent the photoaffinity label from binding nonspecifically without decreasing the effectiveness of the label to bind at the receptor

site. We have utilized sodium salicylate for this purpose. Its use-
fulness in decreasing nonspecific binding of ferric D-parabactin to
membrane preparations will be demonstrated in the following section.
Unfortunately photolysis in the presence of salicylate resulted in a
similar degree of nonselectivity. Other modifications in the photo-
labeling experiments were made in an attempt to increase the selec-
tivity and efficiency of the photolabeling. These included photo-
lysis of membrane components prepared with or without detergent as
well as photolysis at different wavelengths. In all instances the
same degree of nonselectivity was observed. While the parabactin
photoaffinity label has not been as successful as hoped, the results
do direct attention to the high molecular weight proteins present in
membrane preparations of _Paracoccus denitrificans_. Their nature and
potential role as membrane receptors will be the topic of further in-
vestigation in the following section. Finally it should be noted
that a photoaffinity label for the siderophore-mediated iron trans-
port system in _Neurospora crassa_ has recently been synthesized.[99]
The label is a derivative of the coprogen class of hydroxamate sider-
ophores. The synthesis was accomplished by reacting coprogen B,
which contains a primary amino group, with the commercially available
N-hydroxysuccinimide active ester of 4-azido-benzoic acid. In the
absence of light the photoaffinity label was shown to be taken up by
the iron transport system in _Neurospora crassa_ similarly to the
natural product. It was also shown to be a competitive inhibitor of
coprogen uptake, $K_I = 5 \, \mu M$, in the dark. The researchers have
proposed the use of the photoaffinity label in the identification of
the siderophore receptor protein in _Neurospora crassa_.

EXTRACTION, ASSAY AND PROPERTIES OF A FERRIC PARABACTIN
OUTER MEMBRANE RECEPTOR IN *Paracoccus denitrificans*

Introduction

A great deal of interest has been raised as a result of recent
findings which demonstrated that iron-regulated outer membrane pro-
teins are expressed by pathogenic bacteria *in vivo* during infec-
tion.[100-104] *Pseudomonas aeruginosa* isolated directly from the lungs
of a cystic fibrosis patient was shown to express iron-regulated
outer membrane proteins.[100] Bacterial isolates from the urine of
patients with urinary tract infection have also been shown to express
these proteins.[102,104] Some of these low-iron induced proteins have
been shown to function as specific receptor proteins for ferric
siderophores. The finding that siderophore receptors are surface
exposed has led investigators to speculate on the feasibility of
vaccine production specific for the outer membrane proteins.[105] If
successful these anti-siderophore receptor antibodies would be
expected to block siderophore-mediated iron uptake in the bacteria
resulting in a decreased metabolic state.

Preliminary investigations have demonstrated the presence of
naturally occurring antibodies in human sera which react with the
iron-regulated outer membrane proteins of *E. coli*.[41] One of these
proteins is the receptor for the siderophore, ferric enterobactin.
Antiserum raised to this ferric siderophore receptor protein has also
been shown to react with iron-inducible proteins in *Salmonella*
typhimurium and *Klebsiella pneumoniae*, species capable of producing

enterobactin. This suggests that the antigenic properties and molecular homology of the ferric enterobactin receptor protein are highly conserved.[41]

Little is known regarding the physical characteristics of ferric siderophore receptor proteins with the exception of the _E. coli_ ferric enterobactin receptor protein. Obviously, more research is warranted regarding the physical characteristics of other bacterial siderophore receptor proteins, beginning with their identification and isolation. In the present study we furnish direct evidence for the existence of a siderophore binding protein in the outer membrane of _Paracoccus denitrificans_. High affinity, stereospecific binding activity for ferric L-parabactin to isolated membrane components is demonstrated. The physical characteristics of the ferric siderophore binding protein has been investigated including an apparent dissociation constant as well as pH and ionic strength effects on binding affinity. Purification of the membrane receptor binding protein has been effected utilizing a detergent extraction procedure in connection with anion-exchange chromatography.

Materials and Methods

General

$^{55}FeCl_3$, specific activity 43.57 Ci/g, in 0.5 M HCl and Biofluor Scintillation Cocktail were purchased from New England Nuclear. Sephadex G 25-50, ethylene diamine di-_o_-hydroxyphenylacetic acid (EDDA), deoxyribonuclease I (D-4527), and ribonuclease A (R-5125) were purchased from Sigma Chemical Co. EDDA was deferrated and purified according to the method described by Rogers.[106] Triton X-100 was

obtained from Serva Biochemicals Inc. Acrylamide and ammonium sulfate were obtained from Schwarz/Mann Biotech. Gallium (III) nitrate nonahydrate was purchased from Alfa. D-Parabactin was synthesized and purified in a manner identical to L-parabactin but using D-BOC-Threonine instead of L-BOC-Thr.[28] [^{3}H]-L-Parabactin was prepared analogously, starting with [^{3}H]-L-threonine. Final specific activity was 10.5 x 10^3 dpm/µg. Salicylic acid was twice recrystallized from hot 0.01 N HCl and sublimed at 70°C in high vacuum.

Bacterial Strain and Culture Conditions

Paracoccus denitrificans (ATCC Strain 19367) was maintained on trypticase agar plates. Individual colonies were inoculated into 20 mL of trypticase soy broth and incubated with rotary shaking for 24 h at 30°C. Inoculations were then made into a low-iron minimal salts liquid media at 200 µL broth inoculum per 100 mL and incubated with shaking at 30°C. The low-iron minimal salts media was prepared as previously described,[19] but with the addition of 0.2 mg/mL EDDA and 0.5% Tween 80. Cells were harvested when turbidometric optical densities were between 0.10 and 0.16 as determined by a Klett-Summeron colorimeter (A.H. Thomas Co.).

Protein Determination

Protein concentration was estimated using bovine serum albumin as the standard by the method of Lowry et al.[107] with modifications for membrane protein samples as described by Markwel et al.[108]

Isolation of Membranes

Cells of middle to late log phase (3-5 mg protein per mL) were harvested by centrifiguation at 7000 x g for 25 min at 4°C, and twice washed in 50 mM Tris HCl, pH 7.5 containing 10 mM MgCl$_2$, DNase (1 μg/mL), and RNase (1 μg/mL) to give a thick suspension. The cells were resuspended to a volume of 40 mL and homogenized by two passages through a prechilled French pressure cell (18,000 psi). After sitting for an additional 30 min at 4°C, the crude homogenate was centrifuged at 5000 x g for 30 min at 4°C to remove unbroken cells and large debris. The resulting supernatant was carefully removed and ultracentrifuged at 105,000 x g for 60 min at 4°C to isolate the cell envelopes. The high speed supernatant was designated to be soluble "cytosol" proteins. The pellet was resuspended in 50 mM Tris HCl, pH 7.5 to a protein concentration between 10 and 20 mg/mL to give a yellow-green liquid which could be stored at 4°C for at least two weeks without formation of sediment or apparent loss of binding activity. This preparation was designated to be whole cell "membranes."

Extraction of Membrane Proteins

Solubilized protein extracts selectively enriched in inner (cytoplasmic) or outer (cell wall) membrane components were prepared based on a method described by Schnaitman.[109] The membranes were pelleted at 105,000 x g, then resuspended and extracted with 100 mM Tris HCl, pH 7.5 containing 2% Triton X-100 and 10 mM MgCl$_2$. In this and subsequent operations, volumes were adjusted to achieve working protein concentrations of ca. 5 mg/mL of suspension. This

suspension was incubated 1 h at 4°C and centrifuged at 105,000 x g, for 60 min at 4°C. The supernatant was designated the "Mg^{+2} TX-100 extract." The Mg^{+2} TX-100 extracted pellet was then resuspended and extracted with 100 mM Tris HCl, pH 7.5 containing 2% Triton X-100 and 5 mM EDTA. After incubation at 4°C for 1 h, the EDTA Triton X-100 suspension was centrifuged at 105,000 x g for 60 min at 4°C. The supernatant, designated the "EDTA TX-100 extract," contained solubilized outer membrane proteins and displayed the highest specific activity for binding ferric parabactin. Treatment of the "EDTA TX-100 extract" with ammonium sulfate at 80% saturation at 4°C for 2 h salted out the proteins which, after centrifugation, formed a mass which floated on top of the solution. This mass was isolated and redissolved in 50 mM Tris HCl, pH 7.5 containing 0.4% Triton X-100 but no EDTA. The resulting solution was adjusted to a protein concentration of 4-5 mg/mL and filtered through a 0.45 μm membrane to give a crystal clear, almost completely colorless solution (in contrast to previous steps which had a yellow-green tinge). This solution was designated as "solubilized receptor" preparation and was stored at 4°C.

Preparation of Iron (III) Parabactin Chelate

In a typical preparation of 1 mL of 20 μM Fe (III) parabactin chelate, 13 μg (21 nmoles) L- or D-parabactin in 26 μL methanol is placed in a 1.5 mL polypropylene microfuge tube and blown dry under a gentle stream of nitrogen. The residue is then dissolved in 69 μL (690 nmoles) 0.01 N NaOH which had been thoroughly deoxygenated and

stored under argon. After the residue is completely dissolved, the solution is diluted with 100 µL deoxygenated water and 1.117 µg (20 nequiv) iron (III) in 30 µL is added. Typically the iron solution is prepared by diluting an atomic absorption standard (1000 µg Fe/mL in 2% HNO$_3$; Aldrich) with water. Thus, the 30 µL of iron solution contained ca. 350 nanoequivalents of H$^+$. The solution should contain excess base at this point [690-5(21)-350 = 235 nequiv OH$^-$]. The purple chelate solution is diluted to 1 mL with 800 µL 100 mM Tris Cl, pH 7.5. It is now important to first centrifuge the solution at 10,000 x g for 5 min, then filter the supernatant through a 0.2 µm membrane in order to remove any ferric hydroxide present. The iron (III) parabactin in 100 mM Tris Cl, pH 7.5 gives a linear Beer's plot over the concentration range 5-200 µM with a molar absorptivity of 1.20 x 10^4 at 332 nm. The gallium (III) chelate of parabactin may be prepared exactly as for that of iron (III) except that it is colorless.

Sephadex G-25 Column-Centrifiguation Binding Assay

A method modified from that described by Penefsky[110] was used to evaluate ferric parabactin binding activity. A 20 mg (± ca. 10%) plug of silylated glass wool was packed into the bottom of the barrel of a 1 mL disposable tuberculin syringe. Acid-washed Pyrex glass wool was silylated with 1% chlorotrimethylsilane in toluene (30 min), washed successively with toluene (2X), methanol (3X) and acetone (2X), and dried at 100°C. This pretreatment of the glass wool was essential for reproducible, quantitative recovery of protein in the eluate. The plugged syringe barrel was then placed in a 15 mL

disposable polypropylene centrifuge tube which had a hole punched in the screw cap to accommodate the column. The column was then filled with a thick slurry of Sephadex G-25 which had been preswollen and equilibrated with the binding assay incubation buffer. After allowing the bed to drain dry, the top of the gel is at ca. 0.9 mL. The columns so prepared were then placed in a Sorvall omnicarrier (cat. no. 565) tube carrier and centrifuged for 2 1/2 min at 1000 rpm (ca. 150 x g) in a Sorvall GLC-1 benchtop centrifuge. The top of the gel bed thus compacted should be between the 0.80 and 0.85 mL calibration marks. A 100 µL aliquot of the binding assay mixture is applied directly to the top of the bed and the column is centrifuged into a clean 15 mL tube for 2 1/2 min at 1000 rpm. The free ligand is retained on the gel bed while protein and bound ligand elutes from the column into the bottom of the 15 mL tube. The volume of eluate ranged from ca. 95-100 µL and was transferred in its entirety to a scintillation vial. The tube may then be rinsed with scintillation fluid for quantitative recovery of bound counts.

Control experiments for retention of free ligand consisted of placing on the column and centrifuging 100 µL incubation mixture without protein and containing either 8.8×10^5 cpm [^{55}Fe]-L-parabactin or 2×10^4 cpm ferric [^{3}H]-L-parabactin. Eluates contained 70-180 cpm for [^{55}Fe] or background for [^{3}H] indicating 99.99+% retention of free ligand on the column when the compacted bed level is 0.75 mL or greater and the applied sample volume is 100 µL. Control experiments to demonstrate complete passage of macromolecules into the eluate included ca. 100-200 µg of either blue dextran,

bovine serum albumin, detergent-solubilized <u>Paracoccus</u> <u>denitrificans</u> membrane proteins, or membrane microvesicles (French pressure cell sheared) in 100 µL incubation buffer which was applied to the column and centrifuged. Protein assays of the eluate revealed 95-97% recoveries for membrane vesicles and 99-100% recoveries for soluble proteins so long as bed levels were less than 0.90 mL. Membrane samples which had been subjected to denaturing conditions (e.g. freeze-thaw), however, were often not entirely recovered in the eluate. With proper attention to controls, this column-centrifugation method is suitable for binding studies with native microvesicular <u>Paracoccus</u> <u>denitrificans</u> membranes.

The typical binding assay conditions consist of incubation at room temperature for 1 h a mixture (200-500 µL) of the following composition: 50-200 µg protein; chelate (50 nM-90 µM); 100 mM Tris HCl, pH 7.5; 0.4% Triton X-100 (for solubilized membrane protein preparations; omit for nondetergent treated samples); and 0.25 M sodium salicylate (pH adjusted to 7.5) was typically added to reduce nonspecific binding. At the end of the incubation period, a 50 µL aliquot was removed for scintillation counting to confirm the total amount of radiolabeled ligand present and a 100 µL aliquot was removed for the column-centrifugation assay described above.

In experiments to determine the binding constant (K_d), all mixtures contained 50 nM [^{55}Fe]-L-parabactin of very high specific activity (2.4 mCi/µmole). Data points for higher ligand concentrations were derived from mixtures to which an appropriate amount of unlabeled ferric-L-parabactin had been added. Thus, for example the

1 μM mixture contained 50 nM [^{55}Fe]-L-parabactin and 950 nM fer-
ric L-parabactin. The data were then treated as displacement of
radioactive ligand by nonradioactive ligand according to the method
of Akera and Cheng.[94]

SDS-Polyacrylamide Gel Electrophoresis

Sodium dodecyl sulfate-polyacrylamide gel electrophoresis (SDS-
PAGE) was performed as described by Laemmli.[80] The slab gels
were 1.0 mm thick and consisted of a 4% stacking gel and a 12%
separating gel. Membrane samples were solubilized in sample buffer
at 100°C for 5 min. Electrophoresis was carried out at a constant
current of 30 mA per slab for 4 h. Gels were stained with Coumassie
Blue R250 in 10% (v/v) acetic acid/40% methanol.

Nondenaturing Gel Electrophoresis and Autoradiography

Slab gels were prepared with 3% stacking gel and either a 7.5%
or 10% separating gel as for SDS-PAGE with the exception that gels
contained 0.1% Triton X-100. Detergent was omitted from sample and
running buffers. Samples were electrophoresed at a constant current
of 15 mA per slab for 5 h at 4°C. Membrane preparations were incu-
bated with [^{55}Fe]-L or D-parabactin and electrophoresed. The
gels were not stained for protein, bur rather were dried prior to
autoradiography. For each experiment a twin gel was run in parallel
replacing the [^{55}Fe] parabactin with the nonradiolabeled ligand
and staining for protein instead of performing autoradiography. The
autoradiograms were performed by exposing the dried untreated gels to
Kodak X-Omatic AR film in a Kodak X-Omatic X-Ray cassette for 5-7
days at -70°C.

<center>Results</center>

Demonstration of High Affinity Binding Activity for Ferric L-Parabactin in Paracoccus denitrificans Membranes

The binding assay conditions were developed using whole cell "membranes" prepared from French pressure cell shearing of Paracoccus denitrificans as the source of receptor binding activity. All protein in these preparations is sedimentable by centrifugation at 105,000 x g for 1 h. These preparations are reported[110] to consist of rather uniformly sized microvesicles (ca. 50-100 nm o.d.) of whole cell membranes with an inside-out symmetry (i.e. inner cytoplasmic membrane facing external medium and outer cell wall facing the interior of the vesicle). Attempts to store these preparations frozen at -20°C with or without 20% glycerol resulted in a substantial loss of binding activity. However, membrane preparations adjusted to 5-10 mg protein/mL in 50 mM Tris HCl, pH 7.5 and filtered through a 0.45 μM membrane retain essentially all binding activity after storage at 4°C for two weeks.

The binding assay showed a linear dependence on receptor concentration under the conditions specified (50-200 μg protein/200 μL incubation mixture). Incubation periods ranging from 45 min to 3 h at room temperature yielded similar results. Data from assays done in triplicate typically exhibit standard deviations on the order of ±10% when substantial specific binding activity, e.g. >1000 cpm, is present in the sample. When low binding activity is present standard deviations may typically be ± 25% or larger (corresponding to ± ca. 50-200 cpm).

Initial binding experiments performed with 1 μM [^{55}Fe]-L-para-bactin in 50 mM Tris HCl, pH 7.5 showed that a preparation of whole cell membranes (100 μg) bound ca. 8.6% (8.6 ± 0.6 pmoles) of the [^{55}Fe] in the incubation mixture. In the presence of excess (100 μM) unlabeled ferric L-parabactin, binding was reduced to 1.5% (1.5 ± 0.7 pmoles). Parallel binding experiments with ferric O-parabactin indicated that Paracoccus denitrificans membranes also exhibit stereospecificity. In these experiments in 50 mM Tris HCl, pH 7.5 and 1 μM [^{55}Fe]-O-parabactin, 100 μg of whole cell membranes bound 3.3% (3.3 ± 1.0 pmoles) of the [^{55}Fe] in the incubation mixture. In the presence of excess (100 μM) unlabeled ferric D-parabactin, there was only a modest reduction in this binding to 1.5% (1.5 ± 0.3 pmoles).

Taken together, these data suggested that the Paracoccus denitrificans' membranes exhibit two types of binding activity: (1) a "specific" saturable binding with high affinity and characterized to be stereospecific for ferric L-parabactin and (2) "nonspecific" binding which was nonsaturable (i.e. directly proportional to ligand concentration up to 100 μM) and which was nonstereospecific so that the amount of nonspecific background binding was identical for O- or L-ferric parabactin. A number of ionic conditions in the assay mixture were explored with the goal of optimizing specific binding while minimizing nonspecific binding and maximizing stereospecificity

(Table 4-1). In these examples, binding of $[^{55}Fe]$-L-parabactin was similar under very different ionic conditions, whereas certain conditions such as the presence of 0.25 M sodium salicylate markedly reduced the amount of nonspecific (i.e. $[^{55}Fe]$-D-parabactin) binding. For this reason, we chose subsequently to routinely include 0.25 M sodium salicylate in our incubation mixtures.

Using the optimized assay conditions, the binding of $[^{55}Fe]$-L-parabactin and $[^{55}Fe]$-D-parabactin to <u>Paracoccus denitrificans</u> membranes was examined in triplicate over a broad range of ligand concentrations. The stereospecific, high affinity and the low affinity, nonsaturable, nonstereospecific binding activities are each clearly demonstrated in these data. At low ligand concentrations (<5μM) the high affinity, stereospecific system recognizing only ferric L-parabactin dominates, whereas, at higher ligand concentrations, this specific system becomes saturated and nonspecific, nonstereospecific binding is observed (Table 4-2). While these data were considered insufficient to reliably assign a value for the K_d of the high affinity binding, it is clear that at concentrations greater than 10 μM the high affinity system no longer makes a measurable contribution to net binding. An apparent upper limit of 1 μM for K_d in microvesicular membranes is indicated.

Solubilization of Ferric L-Parabactin Binding Activity in Apparent Association with Outer Membrane Proteins

The selective detergent extraction scheme of Schnaitman depends on the requirement of divalent cation (e.g. Mg^{2+}) for maintenance of

Table 4-1. Effect of Various Ionic Conditions on $[^{55}Fe]$-L-Parabactin and $[^{55}Fe]$-D-Parabactin Binding in Membrane Microvesicles

Conditions	Binding		
	Ferric-L-Parabactin (pmoles/mg protein)	Ferric-D-Parabactin (pmoles/mg protein)	(L/D)
50 mM Tris HCl, pH 7.5	88	33	2.67
+ 0.9% NaCl	96	24	3.96
+ 0.5 mM Cyanocobalmin	84	50	1.68
+ 1 M Guanidine HCl	86	8.6	10.0
+ 0.25 M Salicylate	90	9	10.0

Ligand concentration = 1.0 μM; 100 μg protein/200 μL incubation mixture.

Table 4-2. Stereospecificity of the Ferric
            Parabactin Binding Activity in
            Paracoccus denitrificans Membrane
            Microvesicles

Ligand Concentration	(L/D)
91 μM	1.0
51 μM	1.0
21 μM	1.0
10 μM	1.0
5 μM	1.2
2 μM	4.0
40 nM	14.0

100 μg membrane protein/200 μL incubation mix-
ture. (L/D) refers to ratio of total bound
counts of $[^{55}Fe]_{E}$L-parabactin at a particular
concentration/$[^{55}Fe]$-D-parabactin bound at
the same concentration.

the integrity of the outer cell membrane in Gram-negative bacteria.
Thus detergent extraction of whole membranes in the presence of
$MgCl_2$ selectively solubilizes inner membrane proteins. The outer
membrane remains largely intact and sediments in the high speed
pellet (Mg^{+2} TX-100 Extracted Pellet). Subsequent treatment of
this pellet with EDTA destabilizes the outer membrane and renders its
components more susceptible to detergent extraction. Thus the EDTA
TX-100 Extract is enriched in outer membrane proteins. Figure 4-1
depicts the results of a typical preparation of solubilized ferric
L-parabactin receptor by this procedure. These results were derived
from the same batch of bacteria. The same qualitative pattern of
enrichment of specific ferric L-parabactin binding activity in asso-
ciation with the outer membrane proteins is reproducible from one
culture batch to another. Firstly, bars 1 and 2 demonstrate that
ferric L-parabactin binding activity is membrane-associated with
relatively little activity present in the "Cytosol" fraction. Bar 3
shows the results from extracting whole membranes with 2% Triton
X-100 in the presence of 10 mM $MgCl_2$. This Mg^{+2} TX-100
extract (bar 3) has a lower specific activity than the parent whole
membranes (bar 2). Extraction of the Mg^{+2} TX-100 pellet with 2%
Triton X-100 containing 5 mM EDTA results in fractions containing the
highest specific activity (bars 4 and 5). The EDTA TX-100 extract
(bar 5) displayed the greatest binding activity with nearly 25% of
the radiolabel bound. These results are consistent with ferric
L-parabactin binding activity in Paracoccus denitrificans to be due
to a receptor protein associated with the outer cell membrane.

Figure 4-1. Binding activity of various membrane
preparations incubated with [^{55}Fe] ferric L-parabactin (1 μM).

Bar 1   Supernatant after centrifugation of crude cell
         homogenates (cytoplasmic proteins).

Bar 2   Pellet recovered from centrifugation of crude cell
         homogenates (whole cell membranes).

Bar 3   Supernatant from treatment of whole cell membranes
         with 2% Triton X-100 and 10 mM MgCl$_2$ (Mg^{+2}
         TX-100 extract).

Bar 4   Pellet recovered after treatment of the Mg^{+2}
         TX-100 pellet with 2% Triton X-100 and 5 mM EDTA
         (EDTA TX-100 extracted pellet).

Bar 5   Supernatant from treatment of the Mg^{+2} TX-100
         pellet with 2% Triton X-100 and 5 mM EDTA (EDTA
         TX-100 extract).
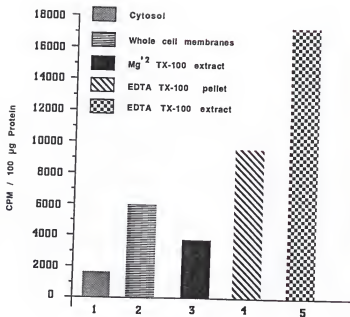
Some Binding Properties of the Detergent
Solubilized Receptor

The binding assay normally used [^{55}Fe] as the radiolabel. The assumption was that the [^{55}Fe] remained in the form of [^{55}Fe]-parabactin chelate and that any counts bound to protein thus represented bound chelate. It was important to demonstrate that this is indeed the case, and, for example, [^{55}Fe] is not stripped from the parabactin ligand so that iron becomes protein-bound in a form not associated with parabactin. We utilized [^{3}H]-L-parabactin to monitor bound ligand. In side-by-side experiments, an equal amount of solubilized protein was assayed for binding of [^{55}Fe]-L-parabactin or [^{3}H]-ferric-L-parabactin. Such experiments demonstrated the same specific activity for binding regardless of which radiolabel was used. Thus for 1 mole of Fe bound there was 1 mole of L-parabactin bound. The gallium (III) [^{3}H]-L-parabactin chelate was also bound well by these preparations. Since Ga (III) cannot be readily reduced under physiological conditions, this argues against a redox stripping of metal from its L-parabactin chelate under binding assay conditions. These results are consistent with a receptor protein recognizing and binding the ferric L-parabactin chelate, then carrying it intact through the column and into the eluate.

An apparent dissociation constant (K_d) for ferric L-parabactin binding to the partially purified Triton X-100 solubilized receptor was estimated as described in Methods by incubating in the presence of 50 nM [^{55}Fe]-L-parabactin of very high specific activity, then adding various amounts of unlabeled ferric L-parabactin (0 to 89.95

μM) to achieve a total ligand concentration range from 50 nM to 90μM. Data were then treated as displacement of [^{55}Fe]-L-parabactin by the unlabeled ferric L-parabactin. The total ligand concentration at which 50% maximal specific binding activity is observed is estimated to be $K_d = 0.7$ μM (Fig. 4-2).

The effects of pH on ferric L-parabactin binding from pH 6.0 to 9.0 were determined at a ligand concentration of 0.5 μM. Duplicate assays were performed at pH 6.0, 6.5, 7.0, 7.5 and 8.0 in a 50 mM Tris-50 mM maleate-NaOH buffer system and at pH 7.0, 7.5, 8.0, 8.5 and 9.0 in a 100 mM Tris-HCl buffer. The values in Table 4-3 demonstrate remarkably little effect of pH on binding under the specified conditions over the pH range 6.0 to 9.0.

The effect of iron-deprivation on the membrane protein composition of Paracoccus denitrificans was determined by comparing the SDS-PAGE profiles of cells grown in the presence or absence of EDDA. As shown in Figure 4-3, whole cell "membranes" prepared from cells grown in the presence of EDDA contained appreciable amounts of protein in the 80,000 molecular weight region. Cells grown in the absence of the synthetic iron-chelator expressed these proteins to a far lesser degree. There were no other significant changes in the protein composition of whole cell "membranes" as a result of iron-deprivation. The induction of these high molecular weight proteins in response to iron-deficient conditions is a confirmation of the work presented by Wilkinson et al.[111]

We have also examined the SDS-PAGE profiles of various membrane preparations obtained from the Schnaitman purification scheme,
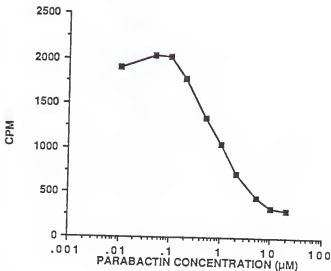
Figure 4-2. Determination of dissociation constant. Data points were obtained on samples containing 50 nM [^{55}Fe] ferric L-parabactin to which an appropriate amount of unlabeled ferric L-parabactin had been added.

Table 4-3. Effects of pH on Ferric L-Parabactin Binding

pH	cpm Bound (Tris-Maleate-NaOH)	cpm Bound (Tris-HCl)
6.0	$20,553 \pm 510$	
6.5	$21,886 \pm 203$	
7.0	$19,899 \pm 829$	$20,563 \pm 578$
7.5	$19,752 \pm 504$	$18,327 \pm 1680$
8.0	$18,966 \pm 300$	$21,106 \pm 200$
8.5		$18,874 \pm 314$
9.0		$23,662 \pm 301$

Ligand concentration = 500 nM [^{55}Fe]-L-parabactin; 150 µg protein/200 µL incubation mixture; incubate 1 h at 20°C. Data presented as mean and range of duplicate assays.
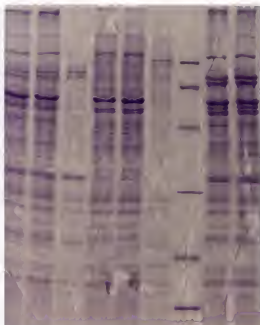
Figure 4-3. Induction of outer membrane proteins in <u>Paracoccus denitrificans</u> in response to iron deprivation.

Lanes 1-2   Cells grown in minimal salts media.
Lanes 8-9   Cells grown in minimal salts media containing EDDA.
Lane 7   SDS standards: Phosphorylase B (92,500), bovine serum albumin (66,200), ovalbumin (45,000), carbonic anhydrase (31,000), soybean trypsin inhibitor (21,500) and lysozyme (14,400).

with special attention made to the low-iron inducible proteins (Fig. 4-4). An absence of these iron-regulated proteins in the soluble "cytosol" fraction and the "Mg^{+2} TX-100 extract" is revealed. These fractions were shown to exhibit the least amount of binding activity as determined by the column centrifiguation assay. The presence of the iron-regulated proteins in the whole cell "membranes," "EDTA TX-100 pellet" and "EDTA TX-100 extract" reveals an association with the outer membrane. These fractions exhibited the greatest degree of binding activity. The enrichment of the 80,000 molecular weight proteins in the "EDTA TX-100 extract" demonstrates the effectiveness of the Schnaitman procedure in the solubilization and partial purification of these proteins.

To further characterize the membrane protein(s), in _Paracoccus denitrificans_ responsible for siderophore binding, experiments were performed to visualize binding of ferric parabactin to membrane preparations. Initial attempts involved the incubation of whole cell "membranes" with [^{55}Fe] labeled L- or D-parabactin. Protein samples were then subjected to SDS-PAGE in the presence or absence of mercaptoethanol and heat. Unfortunately, there was no association of radiolabel with any of the protein bands as detected by autoradiography. With the possibility that the receptor binding protein was no longer functional in the presence of the strong denaturing detergent experiments were performed using the milder nonionic detergent, Triton X-100. Whole cell "membranes" (150 µg) were incubated with 5 µM [^{55}Fe] labeled L- or D-parabactin at room temperature for 30 min.
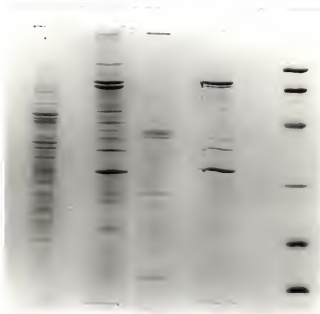
Figure 4-4. SDS-PAGE profile of the various membrane preparations of _Paracoccus denitrificans_ recovered from the Schnaitman purification scheme.

Lane 1   Cytoplasmic proteins
Lane 2   Whole cell membranes
Lane 3   Mg^{+2} TX-100 extract
Lane 4   EDTA TX-100 extract
Lane 5   SDS standards: Phosphorylase B (92,500), bovine serum albumin (66,200), ovalbumin (45,000) and carbonic anhydrase (31,000).

Samples (30-50 μg) were then applied to a nondenaturing polyacrylamide gel and electrophoresed at 4°C. Figure 4-5 demonstrates the resulting autoradiograph from whole "membranes" which had been separated on a 10% acrylamide resolving gel. The association of radiolabel with discrete protein bands of low mobility is evident. Additionally, one band exhibits a very marked stereospecificity appearing very intense in the presence of $[^{55}Fe]$-L-parabactin (Lane 3) and very faint in the presence of $[^{55}Fe]$-D-parabactin (Lane 4). An interesting observation is that D-parabactin is apparently binding specifically to a protein of lower mobility. The nature of this binding is unclear at the present time. An interesting explanation is that we are observing binding to a protein which is involved in the processing of ferric L-parabactin. This processing could include hydrolysis of parabactin to the open chain form which exists in the Δ-coordination isomer and could involve a protein which recognizes this coordination isomer.

We have also examined the binding of $[^{55}Fe]$ labeled L- or D-parabactin to various membrane preparations. As determined from the column-centrifugation assay, procedures which selectively solubilized outer membrane components resulted in preparations containing the highest binding activity. This "EDTA TX-100 extract" was incubated with $[^{55}Fe]$-L-parabactin, then electrophoresed on a polyacrylamide gel containing a 7.5% resolving gel. The autoradiograph (Fig. 4-6) reveals the presence of radiolabel associated with a single protein band (Lanes 1 and 5). In addition when the EDTA pelleted fraction was incubated with $[^{55}Fe]$-L-parabactin there was association of

Figure 4-5. Autoradiographs of whole cell membranes incubated with [^{55}Fe] ferric L-parabactin or D-parabactin.

Gel containing 10% acrylamide and 0.2% Triton.

Lane 1   Samples stored at -20°C, incubated with [^{55}Fe] L-parabactin.
Lane 2   Samples stored at -20°C, incubated with [^{55}Fe] D-parabactin.
Lane 3   Samples stored at 4°C, incubated with [^{55}Fe] L-parabactin.
Lane 4   Samples stored at 4°C, incubated with [^{55}Fe] D-parabactin.

Figure 4-6. Autoradiographs of membrane preparations incubated with [^{55}Fe] ferric L-parabactin or D-parabactin.

Gel containing 7% acrylamide and 0.2% Triton.

Lanes 1,5 EDTA TX-100 extract incubated with [^{55}Fe] L-parabactin.
Lane 2 Whole membranes incubated with [^{55}Fe] D-parabactin.
Lane 3 EDTA TX-100 pellet incubated with [^{55}Fe] L-parabactin.
Lane 4 EDTA TX-100 pellet incubated with [^{55}Fe] D-parabactin.

radiolabel with this same protein band (Lane 3). In contrast the
incubation of various membrane preparations with [^{55}Fe]-D-parabactin
did not result in an association of radiolabel with this same protein
band (Lanes 2 and 4). To determine the molecular weight of the
protein responsible for binding ferric L-parabactin, we excised a
Coomassie Blue stained nondenaturing gel slice which corresponded to
the protein band which had incorporated radiolabel in the 10%
acrylamide gel. Figure 4-7 (Lanes 4 and 5) demonstrates the profile
when this gel slice was subjected to SDS-PAGE. Interestingly, the
major protein in the SDS profile is apparently the low iron inducible
80,000 molecular weight protein.

Various modifications in the detergent extraction procedure
were employed in the hope of increasing the yield of the low-iron
induced proteins in the "EDTA TX-100 extract" to facilitate their
isolation. It was observed that incorporating 0.4% Triton X-100
rather than 2% in the extraction procedure resulted in a preparation
containing increased amounts of the upper band in the 80,000
molecular weight range relative to the lower protein band in this
region (Fig. 4-8). The resulting "EDTA-extract" solubilized with
0.4% detergent retained the high-affinity stereospecific binding when
assayed with [^{55}Fe] L-parabactin (Figure 4-9). The specific
activity had actually increased over the binding observed for
preparations solubilized with 2% detergent. Purification of the
low-iron inducible high molecular weight proteins was effected by
chromatography with the anion-exchange resin, DEAE-cellulose. The
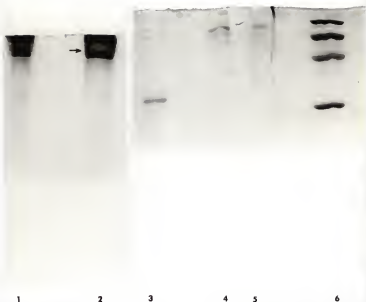
Figure 4-7. SDS-PAGE profile of excised nondenaturing gel slice.

Lanes 1 and 2 - Protein separated on a nondenaturing 10% acrylamide gel.
Lane 3 - Top band from nondenaturing gel separated under SDS-PAGE conditions.
Lanes 4 and 5 - Excised binding protein separated under SDS-PAGE conditions.
Lane 6 - SDS standards: Phosphorylase B (92,500), bovine serum albumin (66,200), ovalbumin (45,000), and carbonic anhydrase (31,000).
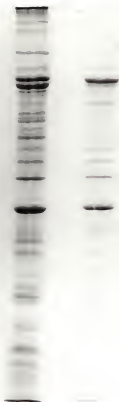
Figure 4-8. Comparison of the EDTA soluble receptor proteins extracted with 0.4% and 2% Triton X-100.
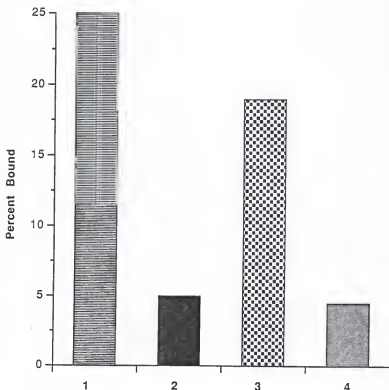
Figure 4-9. Binding activity for "EDTA extracts" solubilized with 0.4 or 2.0% Triton X-100.

Bar 1 EDTA extract (0.4%) incubated with [^{55}Fe] ferric L-parabactin.
Bar 2 EDTA extract (0.4%) incubated with [^{52}Fe] ferric D-parabactin.
Bar 3 EDTA extract (2.0%) incubated with [^{55}Fe] ferric L-parabactin.
Bar 4 EDTA extract (2.0%) incubated with [^{55}Fe] ferric D-parabactin.

EOTA-TX-100 extract preparation solubilized with 0.4% Triton X-100 was dialyzed against 50 mM Tris HCl, pH 7.5, containing 0.4% Triton X-100 and 5 mM EDTA for 24 h. The sample (2 mg) was applied to a column containing DEAE-cellulose (4 mL) which had been equilibrated with the same buffer. After the sample was applied the column was washed with 5 bed volumes of buffer at a flow rate of 2 mL per h. This was followed by a salt gradient of 0 to 100 mM sodium chloride in the same buffer system administered in 6 bed volumes (initiated at fraction 20). A fraction size of 1 mL was collected throughout the experiment. An aliquot (100 µL) from each fraction was removed and precipitated with ammonium sulphate at 80% saturation. Fractions containing protein were then subjected to SDS-gel electrophoresis. Figure 4-10 displays the protein composition of various fractions from the anion-exchange column. The presence of the high molecular weight low-iron inducible proteins as the only major component in the SDS-PAGE profiles (fractions 32-44) demonstrates the effectiveness of this method to selectively purify these proteins (compare Figure 4-8).

All fractions containing the high molecular weight proteins were pooled, then concentrated via ammonium sulphate precipitation, then dialyzed against 50 mM Tris-HCl pH 7.5 containing 0.4% Triton X-100 and 5 mM EDTA. Samples were then incubated with [^{55}Fe] labeled L- or D-parabactin and assayed for binding activity using the column centrifugation technique. This pooled fraction retained the high affinity, stereospecific binding for ferric L-parabactin. Further purification of this preparation was effected with the parabactin affinity column. The column (0.7 mL) was equilibrated with buffer containing 10 mM Tris HCl pH 7.5 and 0.4% Triton X-100 then
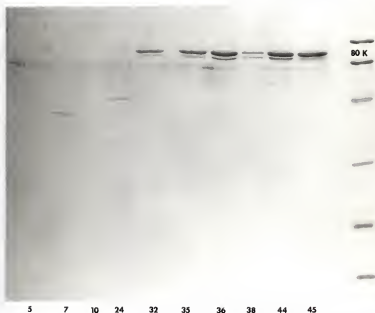
Figure 4-10. SDS-PAGE profile of fractions from the DEAE-cellulose chromatography column demonstrating the purification of the low-iron inducible high molecular weight proteins.

eluted with a sodium chloride gradient. The proteins of interest eluted off the column with 100 mM salt and were substantially cleaner than earlier fractions.

Discussion

In gram-negative bacteria it is a common finding to see the expression of outer membrane proteins in response to iron deficient conditions. For example, in Vibrio cholerae several outer membrane proteins are expressed in cells grown in the absence of iron.[112] In Klebsiella aerogenes at least six new iron regulated outer membrane proteins in the 70,000-80,000 molecular weight region were present in cells grown in iron restricted serum or iron deficient media.[113] The synthesis of three iron-regulated high molecular weight outer-membrane proteins in Campylobacter jejuni has also been reported.[114] In most cases there is no direct evidence linking these iron-regulated proteins in siderophore-mediated iron transport. However, as the production of these proteins is coordinately regulated with the biosynthesis of siderophores in response to iron deprivation, it appears likely that one or more of these proteins serves as a sidero-phore receptor or a component thereof.

In Agrobacterium tumefaciens there is indirect evidence for the existence of a ferric-siderophore receptor. This is relevant to the present investigation as this soil bacterium produces the siderophore agrobactin which is remarkably similar in structure to the Paracoccus denitrificans siderophore, parabactin. Neilands et al.[115] had isolated an Agrobacterium tumefaciens mutation which was unable to

utilize its siderophore in iron-transport. Upon examination of the outer membrane proteins it was observed that the mutation lacked an 80,000 molecular weight protein present in normal cells. Wilkinson et al.[111] have shown that growing Paracoccus denitrificans under iron-deficient conditions also results in the production of outer membrane proteins in the 80,000 molecular weight region. However, there was no information concerning their function, if any, in iron-transport or utilization.

The most compelling evidence for the existence of ferric-siderophore receptors comes from studies with the enteric bacteria E. coli. This microorganism has been shown capable of transporting iron to the cell by no less than four high-affinity iron assimilation pathways.[2] The E. coli receptor protein responsible for the binding of ferric enterobactin has been isolated and character-ized.[79,116] The receptor, a low-iron inducible protein, is referred to as 81 K by its relative subunit molecular weight on SDS-gel electrophoresis. The protein has been isolated to near homogeneity and shown to retain ferric-enterobactin binding activity following solubilization in an EDTA-Triton X-100 containing buffer.[116] The binding assay was performed utilizing a DEAE-cellulose anion exchange resin which separated free and receptor bound ferric-enterobactin. Outer membranes isolated from an E. coli mutation which lacked this 81 K protein were shown to contain no binding activity in the presence of ferric enterobactin.

Additional direct evidence for the existence of ferric siderophore receptors is found in _Pseudomonas aurogenosa_.[117] A low-iron inducible 14,000 molecular weight protein was shown to bind radiolabeled ferric pyochelin as detected by an autoradiographic analysis of SDS-gels. The receptor protein retained this binding activity when transferred to nitrocellulose sheets.

Our results strongly indicate the presence of a ferric parabactin binding protein associated with the outer membrane in _Paracoccus denitrificans_. Binding activity was evaluated by means of a Sephadex G-25 column-centrifugation assay which separated free ligand from protein-bound ligand. Binding was shown to be of the intact [^{55}Fe] ferric parabactin complex to membrane proteins as similar binding data were obtained for tritium labeled ferric parabactin.

Initial experiments with whole cell "membranes" revealed the presence of saturable, high affinity binding activity in addition to a low affinity nonsaturable binding process. The binding activity was further examined by comparing the ability, of [^{55}Fe]-L-parabactin and [^{55}Fe]-D-parabactin to bind to whole cell "membranes." The finding of substantially greater binding affinity for ferric L-parabactin indicates a high degree of stereospecificity in the membrane protein. This stereospecificity is related to the binding proteins' ability to recognize the metal coordination center of ferric L-parabactin which exists exclusively as the Λ-cis isomer.[19] This confirms our previous finding that D-parabactin was ineffective donating iron to cell suspensions of _Paracoccus denitrificans_ in a high affinity system.[19]

Solubilization of ferric L-parabactin binding activity was effected by the detergent extraction method of Schnaitman. The demonstration of a high degree of binding activity in the "EDTA TX-100 extract" is consistent with the ferric L-parabactin binding protein being associated with the outer cell membrane. The presence of the low iron inducible high molecular weight proteins as a major component in the solubilized membrane preparation containing the highest binding activity suggests that one or more of these proteins is involved in the siderophore-mediated iron-uptake system as a receptor for ferric L-parabactin. Recall also that proteins in this molecular weight range were photolabeled during photolysis with parabactin azide.

Purification of these low-iron inducible proteins was accomplished utilizing anion-exchange chromatography. The resulting purified preparation retained high affinity, stereospecific binding for ferric L-parabactin. The presence of the upper band in the 80,000 molecular weight region as the major protein in this purified preparation suggests it may be the receptor protein for ferric L-parabactin or an essential component in its physiological function.

In the present study we have examined the high affinity system by which _Paracoccus denitrificans_ utilizes its siderophore parabactin in its iron transport apparatus. The results demonstrate the presence of a stereospecific iron transport system inducible by a low concentration of utilizable ferric ion in the cell medium. The siderophore, L-para-bactin, produced by _Paracoccus denitrificans_ under low iron conditions, was able to effectively stimulate growth of the microorganism in iron deplete media. The enantiomer, D-parabactin was ineffective in facil-itating growth stimulation of the microorganism as compared to con-trols. These results indicate that _Paracoccus denitrificans_ recognizes a specific coordination isomer in which the chelating groups are in a left-handed or Λ-coordination propeller about the metal center, as in the case of the ferric L-parabactin chelate and is able to discriminate between the mirror image. The ferric L-parabactin chelate was shown to deliver iron to the microorganism via an "iron-taxi" mechanism in which the siderophore iron complex binds to a membrane receptor where the iron is released and transported into the cell. The deferrated ligand remained extracellular allowing the microorganism to reuse the siderophore in iron transport.

The synthesis of parabactin azide, the first catecholamide sider-ophore photoaffinity label, was accomplished. Its preparation is pred-icated on the generation of ethyl 4-azido-2-hydroxybenzimidate. This imidate is coupled with N^1,N^8-bis(2,3-dihydroxybenzoyl)-N^4-threonyl-spermidine hydrobromide to produce parabactin azide. The photoaffinity

label is shown to have the same biological activity as parabactin in
stimulating the growth of <u>Paracoccus denitrificans</u> when the microorgan-
ism is cultured under low iron conditions. Furthermore, parabactin
azide is shown to form a gallium (III) complex identical with the para-
bactin gallium (III) complex as determined by 300-MHz ^1H NMR. In the
dark parabactin azide promotes iron incorporation into the cell in the
same manner as parabactin i.e., via an "iron-taxi" mechanism. The
evidence also indicates that parabactin azide is able to compete effec-
tively with parabactin for the parabactin receptor site in the absence
of light with an inhibitory concentration, K_I, in the range of 2-5
μM. The data reveal that photolysis of cells in the presence of ferric
parabactin azide resulted in approximately 20% inhibition of iron-up-
take as compared to controls. An autoradiographic analysis of <u>Paracoc-
cus denitrificans</u> membranes photolyzed with [^{55}Fe] ferric parabac-
tin azide reveals an association of radiolabel with high molecular
weight proteins. To determine a possible role in siderophore-mediated
iron transport as receptor proteins a closer examination into the
nature of these high molecular weight proteins was warranted.

We examined the role of isolated <u>Paracoccus</u> <u>denitrificans</u> mem-
brane proteins in siderophore-mediated iron transport. High affinity,
stereospecific binding activity for ferric L-parabactin is shown to be
associated with the cell membrane and not with the soluble cytoplasmic
proteins. Extraction procedures known to selectively solubilize outer
membrane components yielded preparations with the highest binding
activity, while selective solubilization of inner membrane components
gave substantially less active preparations. An absence of the low
iron inducible high molecular weight proteins in the soluble cytoplasmic

fraction and soluble inner membrane fraction was revealed. The fractions containing the low iron inducible proteins exhibited the greatest degree of binding. This was most evident in the EDTA solubilized fraction which demonstrated the highest binding activity. This solubilized preparation was greatly enriched with the high molecular weight proteins. An apparent dissociation constant for ferric L-parabactin binding to the partially purified Triton X-100 solubilized receptor was estimated to be $K_d = 0.7$ μM. The effects of pH on ferric L-parabactin binding from pH 6.0 to 9.0 were determined at a ligand concentration of 0.5 μM and demonstrated remarkably little effect of pH on binding.

Additionally, membrane preparations incubated with [^{55}Fe] L- or D-ferric parabactin were electrophoresed under nondenaturing conditions and binding visualized by an autoradiographic analysis. The identification of discrete bands of radioactivity exhibiting a very marked stereospecificity demonstrates the presence of a ferric L-parabactin receptor protein associated with Paracoccus denitrificans outer membranes.

Purification of the low iron inducible high molecular weight proteins was effected by chromatography with the anion exchange resin DEAE-cellulose. High affinity stereospecific binding was retained for this purified preparation. The presence of the low iron inducible high molecular weight proteins as a major component in the solubilized preparation containing the highest binding activity coupled to the observed binding of the purified proteins indicates very strongly that one or more of these proteins is involved in the siderophore-mediated iron uptake system as a receptor for ferric L-parabactin.

REFERENCES

1. Raymond, K.N.; Carrano, C.J. Acc. Chem. Res. 1979, _12_, 183.

2. Neilands, J.B. Structure and Bonding 1984, _58_, 1.

3. Weinberg, E.D. Microbiol. Rev. 1978, _42_, 45.

4. Bullen, J.J. Rev. of Infect. Dis. 1981, _3_, 1127.

5. Weinberg, E.D. Physiol. Rev. 1984, _64_, 75.

6. Bergeron, R.J.; Elliott, G.T.; Kline, S.T.; Ramphal, R.; St. James, L. Antimicrob. Agents Chemother. 1983, _24_, 725.

7. Lankford, C.E. CRC Crit. Rev. Microb. 1973, _2_, 273.

8. Forsberg, C.M.; Bullen, J.J. Clin. Pathol. 1972, _25_, 65.

9. Neilands, J.B. Annu. Rev. Nutr. 1981, _1_, 27.

10. Neilands, J.B. Structure and Bonding 1972, _11_, 145.

11. Neilands, J.B. "Microbial Iron Metabolism"; Neilands, J.B., Ed.; Academic: New York, 1974.

12. Emery, T. In "Metal Ions in Biological Systems"; Sigel, H., Ed.; Marcel Dekkar: New York, 1978, Vol. 7, p. 77.

13. Neilands, J.B. Annu. Rev. Biochem. 1981, _50_, 715.

14. Keberle, H. Ann. N.Y. Acad. Sci. 1964, _119_, 758.

15. O'Brien, I.G.; Gilson, F. Biochim. Biophys. Acta 1970, _215_, 393.

16. Pollack, J.R.; Neilands, J.B. Biochem. Biophys. Res. Commun. 1970, _38_, 989.

17. Peterson, T.; Falk, K.; Leong, S.; Klein, M.P.; Neilands, J.B. J. Am. Chem. Soc. 1980, _102_, 7715.

18. Harris, W.P.; Carrano, C.J.; Cooper, S.R.; Sofen, S.R.; Ardeef, A.; McArdle, J.V.; Raymond, K.N. J. Am. Chem. Soc. 1979, _101_, 6097.

19. Bergeron, R.J.; Dionis, J.B.; Elliott, G.T.; Kline, S.J. J. Biol. Chem. 1985, _260_, 7936.

20. Ardeef, A.; Sofen, S.R.; Bregante, T.L.; Raymond, K.N. J. Am. Chem. Soc. 1978, 100, 5362.

21. Hider, R.C. Structure and Bonding 1984, 58, 25.

22. Warner, P.J.; Williams, P.H.; Bindereif, A.; Neilands, J.B. Infect. Immun. 1981, 33, 540.

23. Snow, G.A. Bacteriol. Rev. 1970, 34, 99.

24. Tait, G.T. Biochem. J. 1975, 146, 191.

25. Peterson, T.; Neilands, J.B. Tetrahedron Lett. 1979, 50, 4805.

26. Ong, S.A.; Peterson, T.; Neilands, J.B. J. Biol. Chem. 1979, 254, 1860.

27. Griffiths, G.L.; Sigel, S.P.; Payne, S.M.; Neilands, J.B. J. Biol. Chem. 1984, 259, 383.

28. Bergeron, R.J.; Kline, S.J. J. Am. Chem. Soc. 1982, 104, 4489.

29. Bergeron, R.J.; McManis, J.S.; Dionis, J.B.; Garlich, J.R. J. Org. Chem. 1985, 50, 2780.

30. Bergeron, R.J.; Garlich, J.R.; McManis, J.S. Tetrahedron 1985, 41, 507.

31. Pollack, J.R.; Ames, B.N.; Neilands, J.B. J. Bacteriol. 1970, 104, 635.

32. Neilands, J.B. Bacteriol. Rev. 1957, 21, 101.

33. Lankford, C.E. CRC Crit. Rev. Microbiol. 1973, 2, 273.

34. Carnahan, J.E.; Castle, J.E. J. Bacteriol. 1958, 75, 121.

35. Wang, C.C.; Newton, A. J. Bacteriol. 1969, 98, 1135.

36. Davis, W.B.; McCauley, M.J.; Byers, B.R. J. Bacteriol. 1971, 105, 589.

37. Garibaldi, J.A. J. Bacteriol. 1972, 110, 262.

38. Garibaldi, J.A. J. Bacteriol. 1971, 105, 1036.

39. Kochan, I. In "Microorganisms and Minerals"; Weinberg, E.D., Ed.; Marcell Dekker: New York, 1977, p. 251.

40. Yancey, R.J.; Breeding, S.L.; Lankford, C.E. Infect. Immun. 1979, 24, 174.

41. Chart, H.; Griffiths, E. J. of Gen. Microbiol. 1985, 131, 1503.

42. Payne, S.M.; Finkelstein, R.A. J. Clin. Invest. 1978, 61, 1428.

43. Warner, P.J.; Williams, P.H.; Bindereif, A.; Neilands, J.B. Infect. Immun. 1981, 33, 540.

44. Konopka, K.; Neilands, J.B. Biochem. 1984, 23, 2122.

45. Konopka, K.; Bindereif, A.; Neilands, J.B. Biochem. 1982, 21, 6503.

46. Peters, T. In "The Plasma Proteins"; Putnam, F.; Ed., Academic Press: New York, 1975, Vol. 1, p. 133.

47. Moore, D.G.; Yancey, R.J.; Lankford, C.E.; Earhart, C.F. Infect. Immun. 1980, 27, 418.

48. Moore, D.G.; Earhart, C.F. Infect. Immun. 1981, 31, 631.

49. Costerton, J.W.; Ingram, J.M.; Cheng, K.J. Bacteriol. Rev. 1974, 38, 87.

50. Halegoua, S.; Inouye, M. In "Bacterial Outer Membranes"; Inouye, M.; Ed.; Wiley: New York, 1979, p. 67.

51. Rogers, H.J. Bacteriol. Rev. 1970, 34, 194.

52. Neilands, J.B. Ann. Rev. Microbiol. 1982, 36, 285.

53. Negrin, R.S.; Neilands, J.B. J. Biol. Chem. 1978, 253, 2339.

54. Hider, R.C.; Drake, A.F.; Kuroda, R.; Neilands, J.B. Naturwissenshaft 1980, 67, 136.

55. Mirelman, D. In "Bacterial Outer Membranes"; Inouye, M., Ed.; Wiley: New York, 1979, p. 115.

56. Braun, V.; Rehn, K. Eur. J. Biochem. 1969, 10, 426.

57. Costerton, J.W. Rev. Can. Biol. 1970, 29, 299.

58. Nikaido, H.; Vaara, M. Microbiol. Rev. 1985, 49, 1.

59. Smit, J.; Kamio, Y.; Nikaido, H. J. Bacteriol. 1975, 124, 942.

60. Nakae, T. J. Biol. Chem. 1976, 251, 2176.

61. Braun, V.; Hantke, K. In "Organisation of Prokaryotic Cell Membranes"; Gnosh, B.K.; Ed., 1981, Vol. 2, pg. 1.

62. Messenger, A.J.M.; Ratledge, C. J. Bacteriol. 1982, 149, 131.

63. Bergeron, R.J.; Kline, S.J. J. Am. Chem. Soc. 1984, 106, 3089.

64. Neilands, J.B.; Peterson, T.; Leong, S.A. In "Inorganic Chemistry in Biology and Medicine"; Markell, A.E.; Ed., American Chemical Society: Washington, D.C. 1980, p. 263.

65. Nikaido, H. Angew. Chemie. 1979, 91, 394.

66. Kline, S.J. Ph.D. Dissertation, University of Florida, 1984.

67. Carrano, C.J.; Raymond, K.N. J. Bacteriol. 1978, 136, 69.

68. Ratledge, C.; Patel, P.V.; Mundy, J. J. Gen. Microbiol. 1982, 128, 1559.

69. Emery, T. Biochem. 1971, 10, 1483.

70. Ecker, D.J.; Emery, T. J. Bacteriol. 1983, 155, 616.

71. Arceneaux, J.E.L.; Davis, W.B.; Downer, D.N.; Haydon, A.H.; Byers, B.R. J. Bacteriol. 1973, 115, 919.

72. Greenwood, K.T.; Luke, R.K.J. Biochim. Biophys. Acta 1978, 525, 209.

73. Ecker, D.J.; Passavant, C.W.; Emery, T. Biochim. Biophys. Acta 1982, 720, 242.

74. Muller, G.; Winkelmann, G. FEMS Microbiol. Lett. 1981, 10, 327.

75. Emery, T.; Hoffer, P.B. J. Nucl. Med. 1980, 21, 935.

76. Neilands, J.B.; Erickson, T.J.; Rastetter, W.H. J. Biol. Chem. 1981, 256, 3831.

77. Winkelmann, G. FEBS Lett. 1979, 97, 43.

78. Venuti, M.C.; Rastetter, W.H.; Neilands, J.B. J. Med. Chem. 1979, 22, 123.

79. Hollifield, W.C.; Neilands, J.B. Biochem. 1978, 17, 1922.

80. Laemmli, U.K. Nature 1970, 227, 680.

81. Chamberlain, J.P. Anal. Biochem. 1979, 98, 132.

133

82. McGhie, J.R.; Morton, C.; Reynolds, B.L.; Spence, J.W.   J. Soc. Chem. Ind. 1949, 68, 328.

83. Libermann, D.; Rist, N.; Grumbach, F.; Cals, S.; Moyeux, M.; Rouaix, A.   Bull. Soc. Chim. Fr. 1958, 694.

84. Casey, M.L.; Kemp, D.S.; Paul, K.G.; Cox, D.D.   J. Org. Chem. 1973, 38, 2294.

85. Lindemann, H.; Konitzer, H.; Romanoff, S.   Justus Liebigs Ann. Chem. 1927, 456, 284.

86. Knowles, J.R.   Acc. Chem. Res. 1972, 5, 155.

87. Evecinska, M.; Vanderkooi, J.M.; Wilson, D.F.   Arch. Biochem. Biophys. 1975, 171, 108.

88. Hanstein, W.G.   Methods in Enzymology, 1979, 56, 653.

89. Lewis, R.V.; Roberts, M.R.; Dennis, E.A.; Allison, W.S.   Biochem. 1977, 16, 5650.

90. Ji, T.H.   J. Biol. Chem. 1977, 252, 1566.

91. Walker, P.; Waters, W.A.   J. Chem. Soc. 1962, 1932.

92. Lee, G.C.; Waddell, W.H.   J. Org. Chem. 1983, 48, 2897.

93. Abramovitch, R.A.; Challand, S.R.   J. Chem. Soc. Chem. Commun. 1972, 965.

94. Akera, T.; Cheng, V.K.   Biochim. Biophys. Acta 1977, 470, 412.

95. Richards, F.M.; Brunner, J.   Ann. N.Y. Acad. Sci. 1980, 346, 194.

96. Hanstein, W.G.   Methods in Enzymology 1979, 56, 653.

97. Czarnecki, J.; Geahlen, R.; Haley, B.   Methods in Enzymology 1979, 56, 642.

98. Ruoho, A.E.; Kiefer, H.; Roeder, P.; Singer, S.J.   Proc. Natl. Acad. Sci. U.S.A. 1973, 70, 2567.

99. Bailey, C.T.; Hunt, E.M.; Carrano, C.J.; Huschka, H.G.; Winkelmann, G.   Biochim. Biophys. Acta 1986, 883, 299.

100. Brown, M.R.W.; Anwar, H.; Lambert, P.A.   FEMS Microbiol. Lett. 1984, 21, 113.

101. Griffiths, E.; Stevenson, P.; Joyce, P.   FEMS Microbiol. Lett. 1983, 16, 95.

102. Lam, C.; Turnowsky, F.; Schwarzinger, E.; Neruda, W. FEMS Microbiol. Lett. 1984, 24, 255.

103. Sciortino, C.V.; Finkelstein, R.A. Infect. Immun. 1983, 42, 990.

104. Shand, G.H.; Anwar, H.; Kadurugamuwa, J.; Brown, M.R.W.; Silverman, S.H.; Melling, J. Infect. Immun. 1985, 48, 35.

105. Chart, H.; Buck, M.; Stevenson, P.; Griffiths, E. J. Gen. Microbiol. 1986, 132, 1373.

106. Rogers, H.J. Infect. Immun. 1973, 7, 445.

107. Lowry, O.H.; Rosenbrough, N.J.; Farr, A.L.; Randall, R.J. J. Biol. Chem. 1951, 193, 265.

108. Markwell, M.K.; Haas, S.M.; Bieber, L.L.; Tolbert, N.E. Anal. Biochem. 1978, 87, 206.

109. Schnaitman, C.A. J. Bacteriol. 1971, 108, 553.

110. Penefsky, H.S. J. Biol. Chem., 1977, 252, 2891.

111. Hoe, M.; Wilkinson, B.J.; Hindahl, M.S. Biochim. Biophys. Acta 1985, 813, 338.

112. Sigel, S.P.; Payne, S.M. J. Bacteriol. 1982, 150, 148.

113. Williams, P.; Brown, M.R.W.; Lambert, P.A. J. Gen. Microbiol. 1984, 130, 2357.

114. Field, L.H.; Headley, V.L.; Payne, S.M.; Berry, L.J. Infect. Immun. 1986, 54, 126.

115. Leong, S.A.; Neilands, J.B. Infect. Immun. 1981, 147, 482.

116. Fiss, E.H.; Samuelson, P.S.; Neilands, J.B. Biochem. 1982, 21, 4517.

117. Sokol, P.A.; Woods, D.E. Infect. Immun. 1983, 40, 665.

APPENDIX
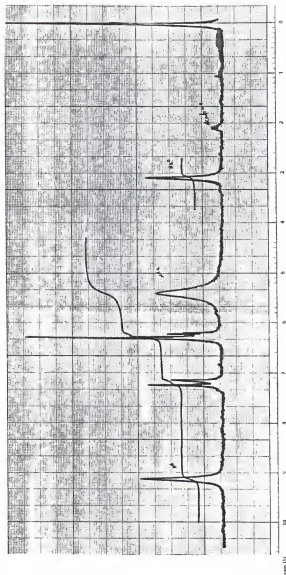
Figure A-1. NMR spectrum of 4-amino-2-hydroxybenzonitrile · HCl (2).
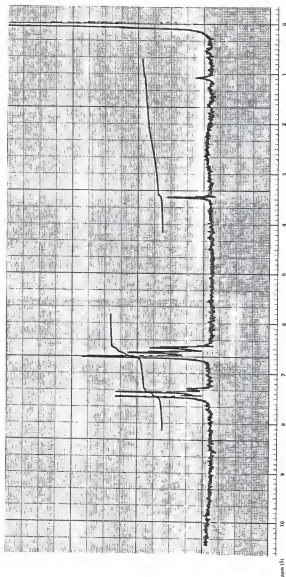
Figure A-2. NMR spectrum of 4-azido-2-hydroxybenzonitrile (3).
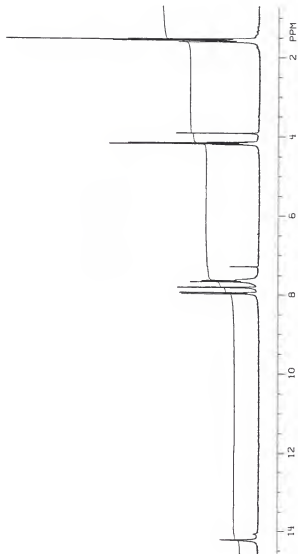
Figure A-3. NMR spectrum of ethyl 2-hydroxy-4-nitrobenzimidate · HCl (5).
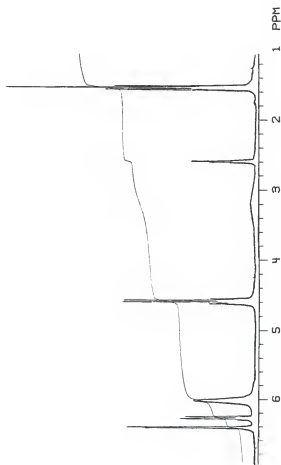
Figure A-4. NMR spectrum of ethyl 4-amino-2-hydroxybenzimidate · HCl (6).
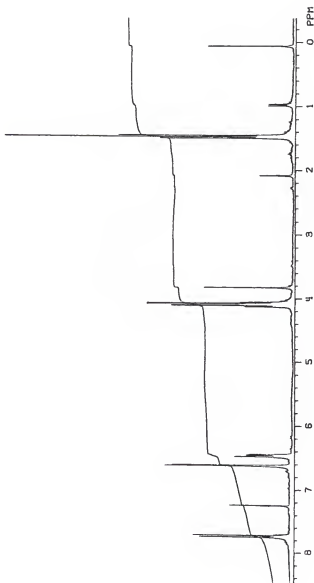
Figure A-5. NMR spectrum of ethyl 4-azido-2-hydroxybenzimidate · HCl (7).
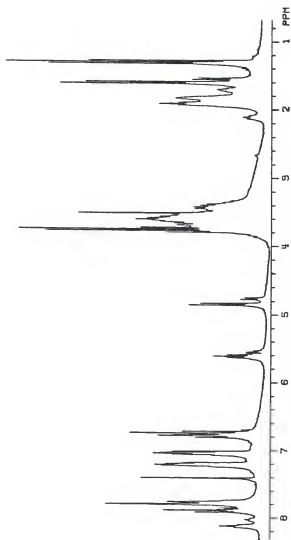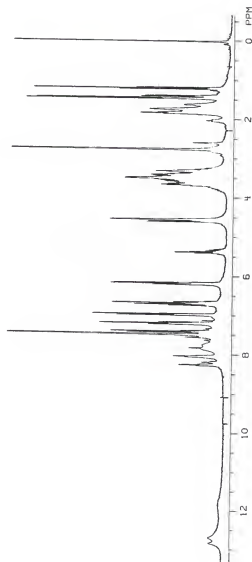
Figure A-6. NMR spectrum of nitroparabactin (8).
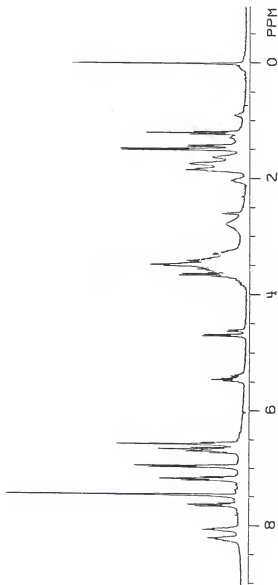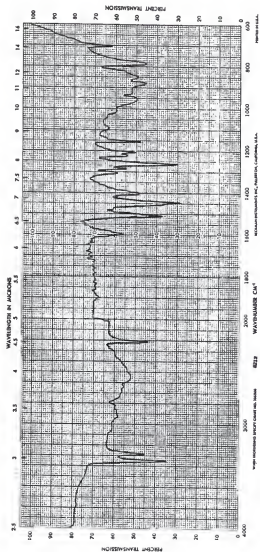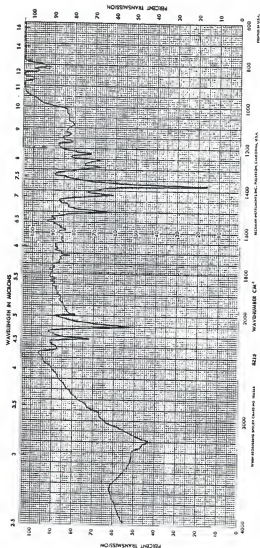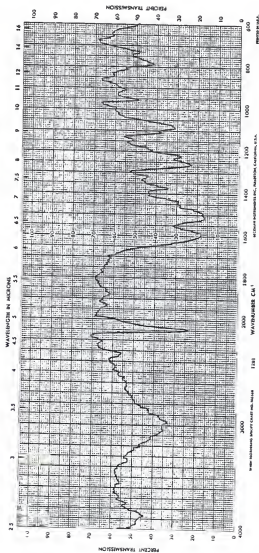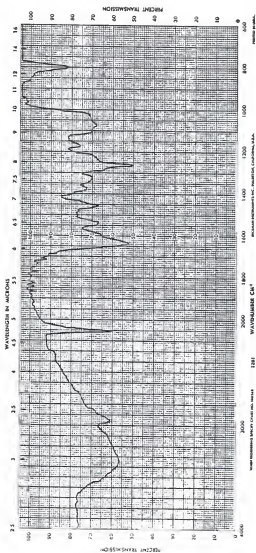
Figure A-7. NMR spectrum of aminoparabactin (9).

Figure A-8. NMR spectrum of parabactin azide (10).

Figure A-9. IR spectrum of 4-amino-2-hydroxybenzonitrile · HCl (2).

Figure A-10. IR spectrum of 4-azido-2-hydroxybenzonitrile (3).

Figure A-11. IR spectrum of ethyl 4-azido-2-hydroxybenzimidate · HCl (7).

Figure A-12. IR spectrum of parabactin azide (10).

John B. Dionis was born in Worcester, Massachusetts, on November 20, 1961. After graduating from Doherty Memorial High School, he enrolled at Clark University where he received his Bachelor of Arts degree in chemistry in May, 1983. The author then entered the graduate program at the University of Florida, Department of Medicinal Chemistry, working under the direction of Dr. Raymond J. Bergeron. After receiving his Ph.D in August, 1987, the author accepted a position as a post doctoral fellow with Ciba-Geigy Limited in Basel, Switzerland.

I certify that I have read this study and that in my opinion it conforms to acceptable standards of scholarly presentation and is fully adequate, in scope and quality, as a dissertation for the degree of Doctor of Philosophy.

Raymond J. Bergeron, Chairman
Professor of Medicinal Chemistry

I certify that I have read this study and that in my opinion it conforms to acceptable standards of scholarly presentation and is fully adequate, in scope and quality, as a dissertation for the degree of Doctor of Philosophy.

Richard R. Streiff, M.D.
Professor of Medicinal Chemistry

I certify that I have read this study and that in my opinion it conforms to acceptable standards of scholarly presentation and is fully adequate, in scope and quality, as a dissertation for the degree of Doctor of Philosophy.

Kenneth B. Sloan
Associate Professor of Medicinal Chemistry

I certify that I have read this study and that in my opinion it conforms to acceptable standards of scholarly presentation and is fully adequate, in scope and quality, as a dissertation for the degree of Doctor of Philosophy.

Stephen G. Schulman
Professor of Pharmaceutical Chemistry

I certify that I have read this study and that in my opinion it conforms to acceptable standards of scholarly presentation and is fully adequate, in scope and quality, as a dissertation for the degree of Doctor of Philosophy.

Charles M. Allen
Professor of Biochemistry and
Molecular Biology

This dissertation was submitted to the Graduate Faculty of the College of Pharmacy and to the Graduate School and was accepted as partial fulfillment of the requirements for the degree of Doctor of Philosophy.

August 1987

Dean, College of Pharmacy

Dean Graduate School